NMR investigations of Polytrifluoroethylene (PTrFE) synthesized by RAFT

Supplementary information

Vincent Bouad[a], Marc Guerre[b], Sami Zeliouche[a], Bruno Améduri[a], Cédric Totée[a], Gilles Silly[a], Rinaldo Poli[c], Vincent Ladmiral[a]*

[a] ICGM, Univ Montpellier, CNRS, ENSCM, Montpellier, France.
[b] Laboratoire des IMRCP, Université de Toulouse, CNRS UMR 5623, Université Paul Sabatier, 118 route de Narbonne, 31062 Toulouse Cedex 9, France.
[c] CNRS, LCC (Laboratoire de Chimie de Coordination), UPS, INPT, université de Toulouse, 205 route de Narbonne, BP 44099, F-31077 Toulouse, Cedex 4, France.

Corresponding author : Address : 8 rue de l'ecole normale, 34090, Montpellier.
E-mail : vincent.ladmiral@enscm.fr

Equation S1 to S4 : Calculations of the relative abundance of the diastereoisomers of each T and H-adduct.

For H-adduct :

$$\text{RS (\%)} = \frac{\int_{-189.0}^{-189.2} CFH}{\int_{-189.0}^{-189.2} CFH + \int_{-203.2}^{-203.4} CFH} * 100 \quad (S1) \; ; \; \text{RR (\%)} = \frac{\int_{-203.2}^{-203.4} CFH}{\int_{-189.0}^{-189.2} CFH + \int_{-203.2}^{-203.4} CFH} * 100 \; (S2)$$

For T-adduct :

$$\text{RS (\%)} = \frac{\int_{-171.0}^{-171.2} CFH}{\int_{-171.0}^{-171.2} CFH + \int_{-173.65}^{-173.85} CFH} * 100 \quad (S3) \; ; \; \text{RR (\%)} = \frac{\int_{-173.65}^{-173.85} CFH}{\int_{-171.0}^{-171.2} CFH + \int_{-173.65}^{-173.85} CFH} * 100 \; (S4)$$

Equation S5 and S6 : Calculation of relative abundance of T and H-adducts.

$$\text{H-Adducts (\%)} = \frac{\int_{-189.0}^{-189.2} CFH + \int_{-203.2}^{-203.4} CFH}{\int_{-171.0}^{-171.2} CFH + \int_{-173.65}^{-173.85} CFH + \int_{-189.0}^{-189.2} CFH + \int_{-203.2}^{-203.4} CFH} * 100 \; (S5)$$

$$\text{T-Adducts (\%)} = \frac{\int_{-171.0}^{-171.2} CFH + \int_{-173.65}^{-173.85} CFH}{\int_{-171.0}^{-171.2} CFH + \int_{-173.65}^{-173.85} CFH + \int_{-189.0}^{-189.2} CFH + \int_{-203.2}^{-203.4} CFH} * 100 \; (S6)$$

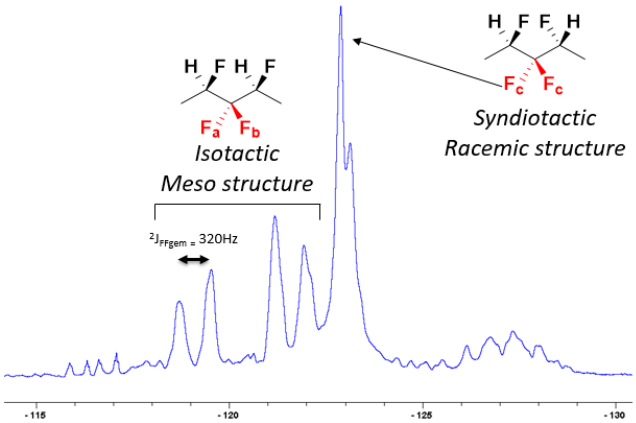

Figure S1. Zoom on [-114 ppm; -131 ppm] region (-CF2-) of the 19F{1H} spectrum of PTrFE made by RAFT (Entry 2, Table 1).

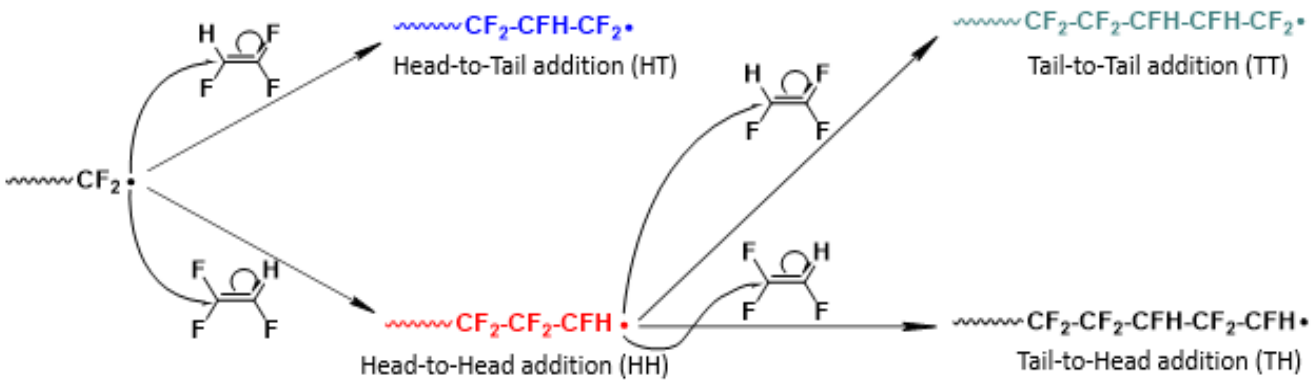

Figure S2. Different possible modes of additions of TrFE depending on the nature of the growing macroradical.

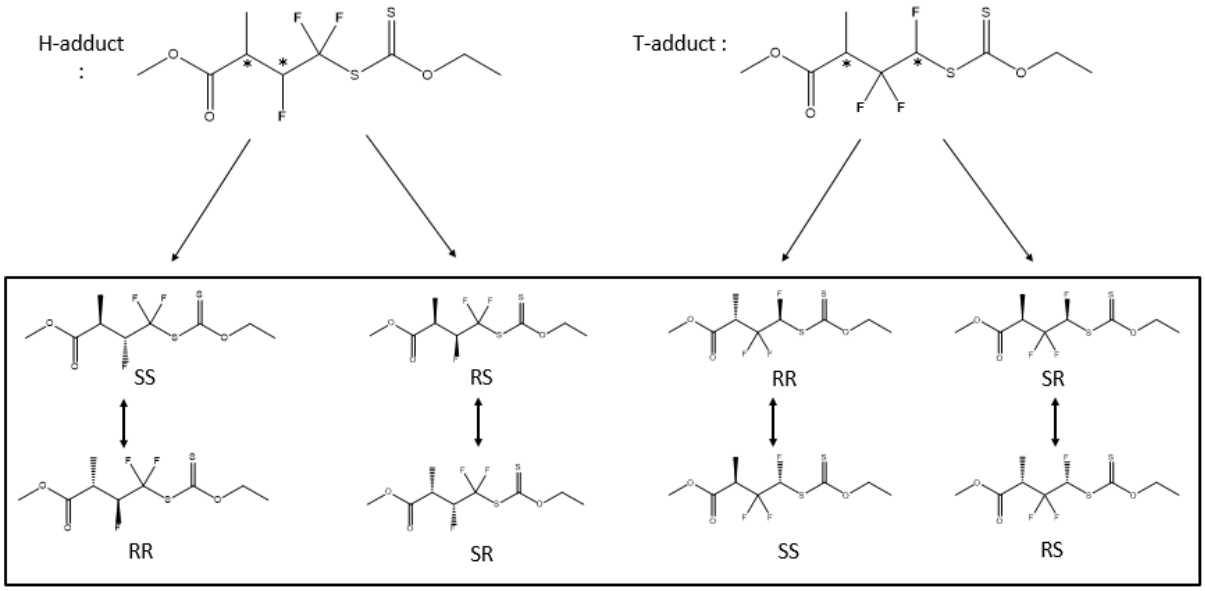

Figure S3. Structures of the enantiomers (indicated by the double-headed arrows) and diastereoisomers pairs for the T- and H-adducts of TrFE and O-ethyl-S-(1-methoxycarbonyl)ethyldithiocarbonate (CTA-XA).

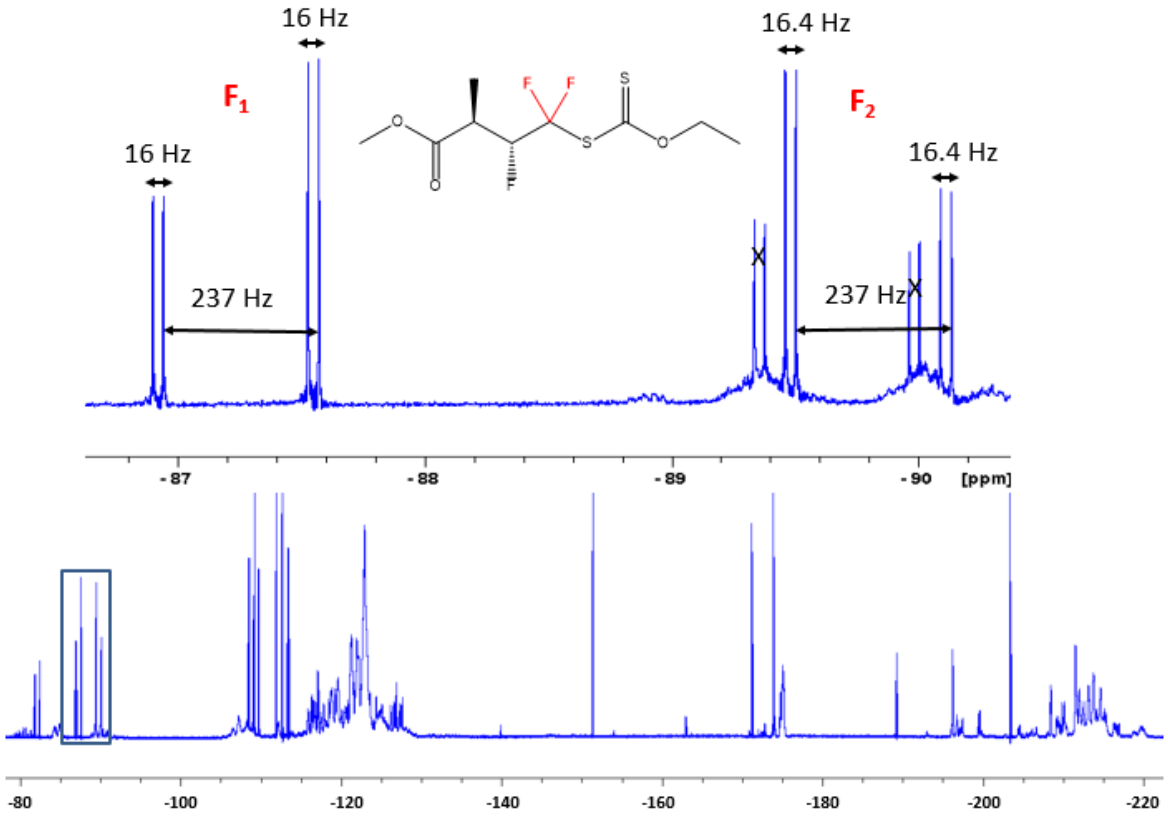

Figure S4. Zoom on $^{19}F\{^{1}H\}$ spectra on the resonance of the CF_2 from the RR/SS diastereoisomer of the H-adduct (Entry 1, Table 1). Note that only the RR stereoisomer is represented but the splitting pattern is identical for the SS stereoisomer.

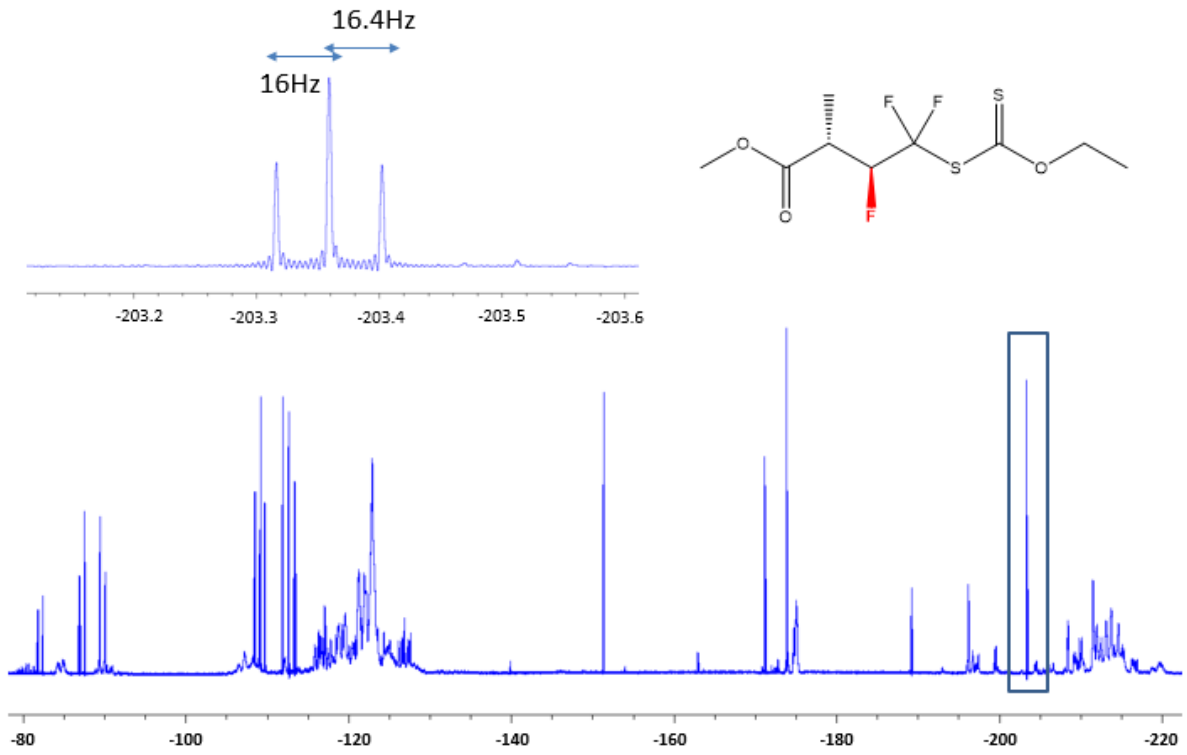

Figure S5. Zoom on $^{19}F\{^{1}H\}$ spectra on the resonance of the CFH from the RR/SS diastereoisomer of the H-adduct (Entry 1, Table 1). Note that the expected doublet of doublet appears as a triplet because of the too small difference of $^{3}J_{F\text{-}F}$ to be seen on the 1D experiment. Only the RR stereoisomer is represented but the splitting pattern is identical for the SS stereoisomer.

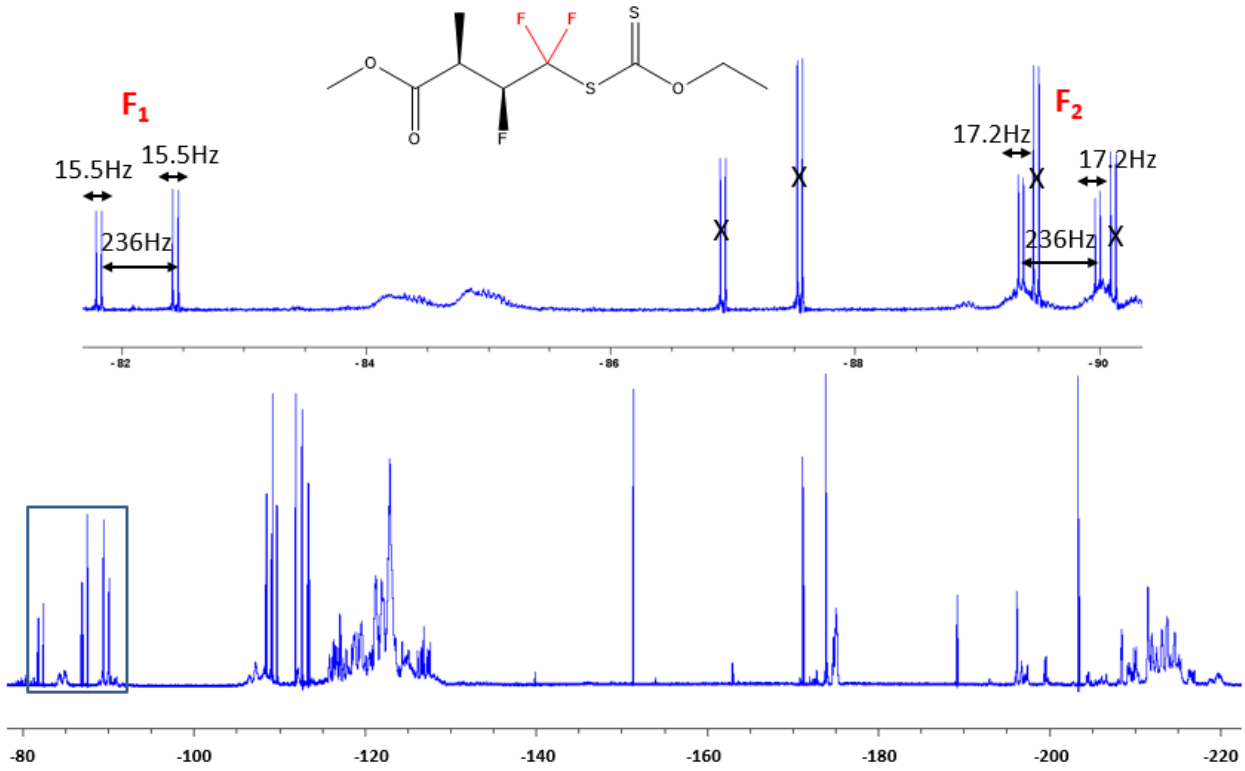

Figure S6. Zoom on $^{19}F\{^{1}H\}$ spectra on the resonance of the CF_2 from the RS/SR diastereoisomer of the H-adduct (Entry 1, Table 1). Only the RS stereoisomer is represented but the splitting pattern is identical for the SR stereoisomer.

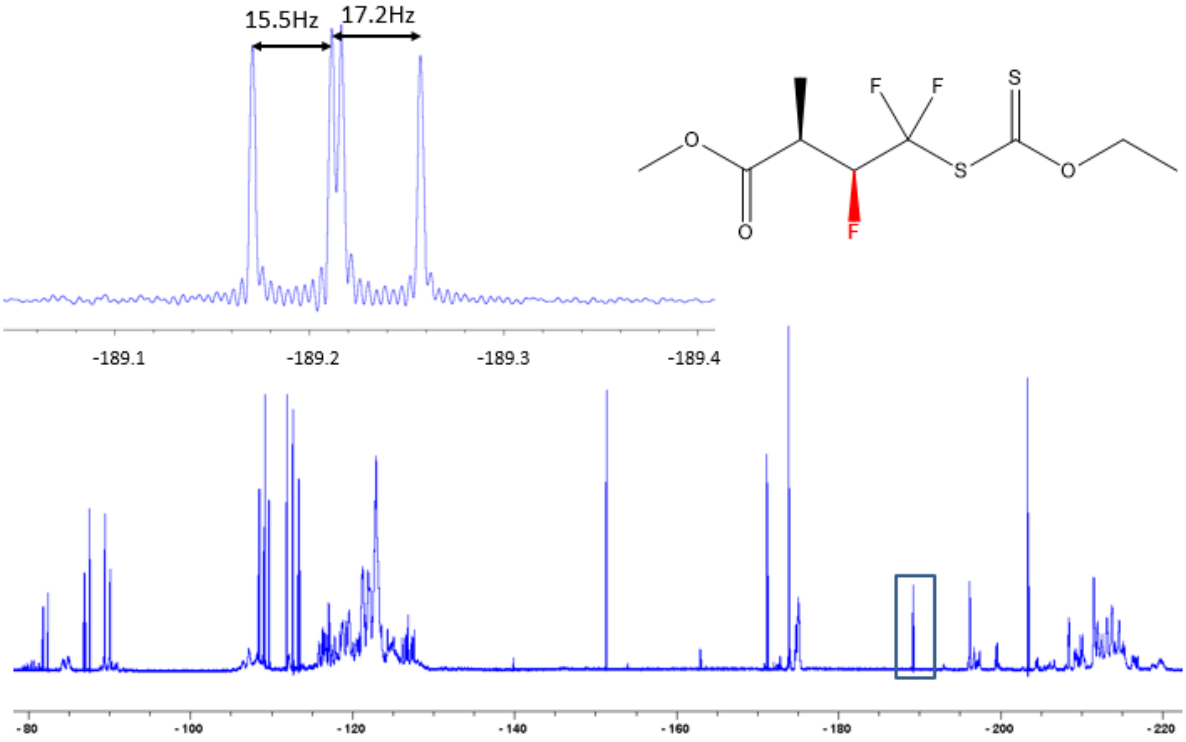

Figure S7. Zoom on $^{19}F\{^{1}H\}$ spectra on the resonance of the CFH from the RS/SR diastereoisomer of the H-adduct (Entry 1, Table 1). Only the RS stereoisomer is represented but the splitting pattern is identical for the SR stereoisomer.

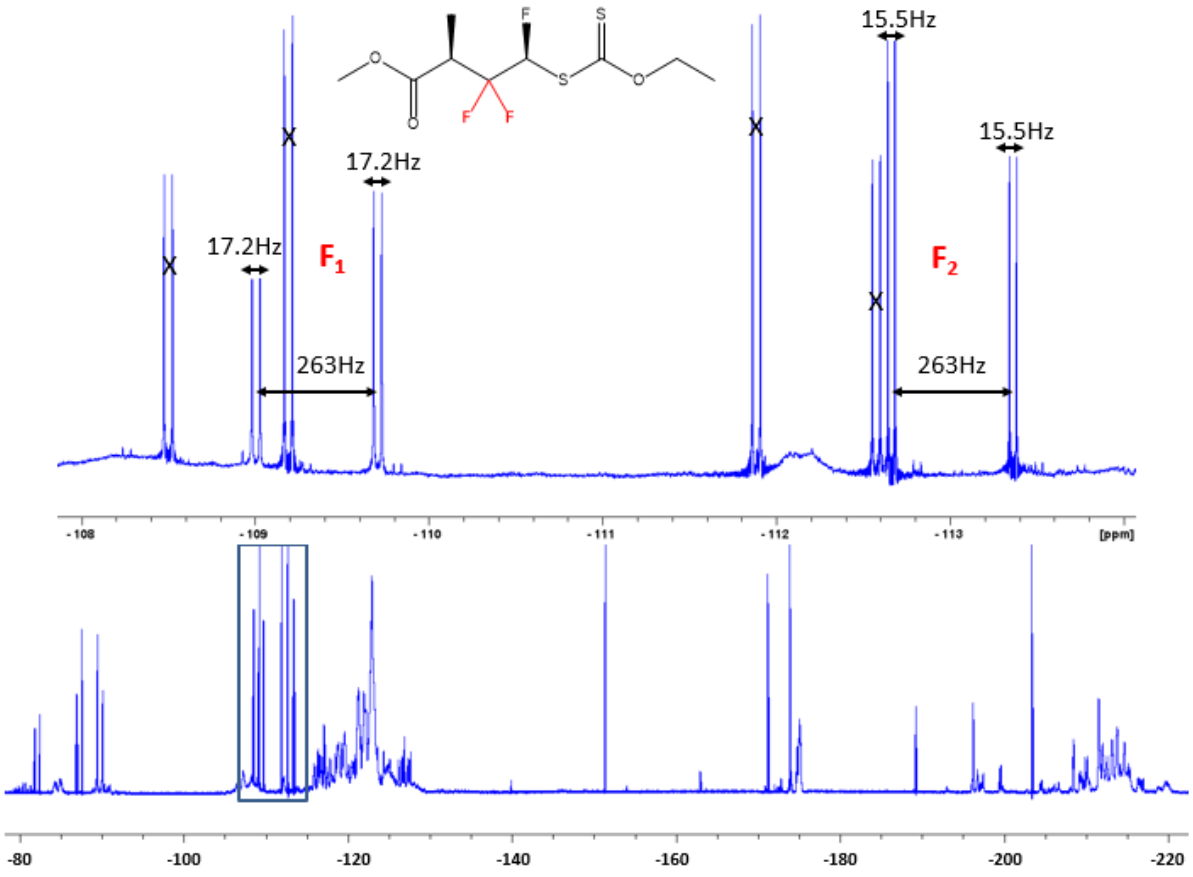

Figure S8. Zoom on $^{19}F\{^{1}H\}$ spectra on the resonance of the CF_2 from the RS/SR diastereoisomer of the T-adduct (Entry 1, Table 1). Only the RS stereoisomer is represented but the splitting pattern is identical for the SR stereoisomer.

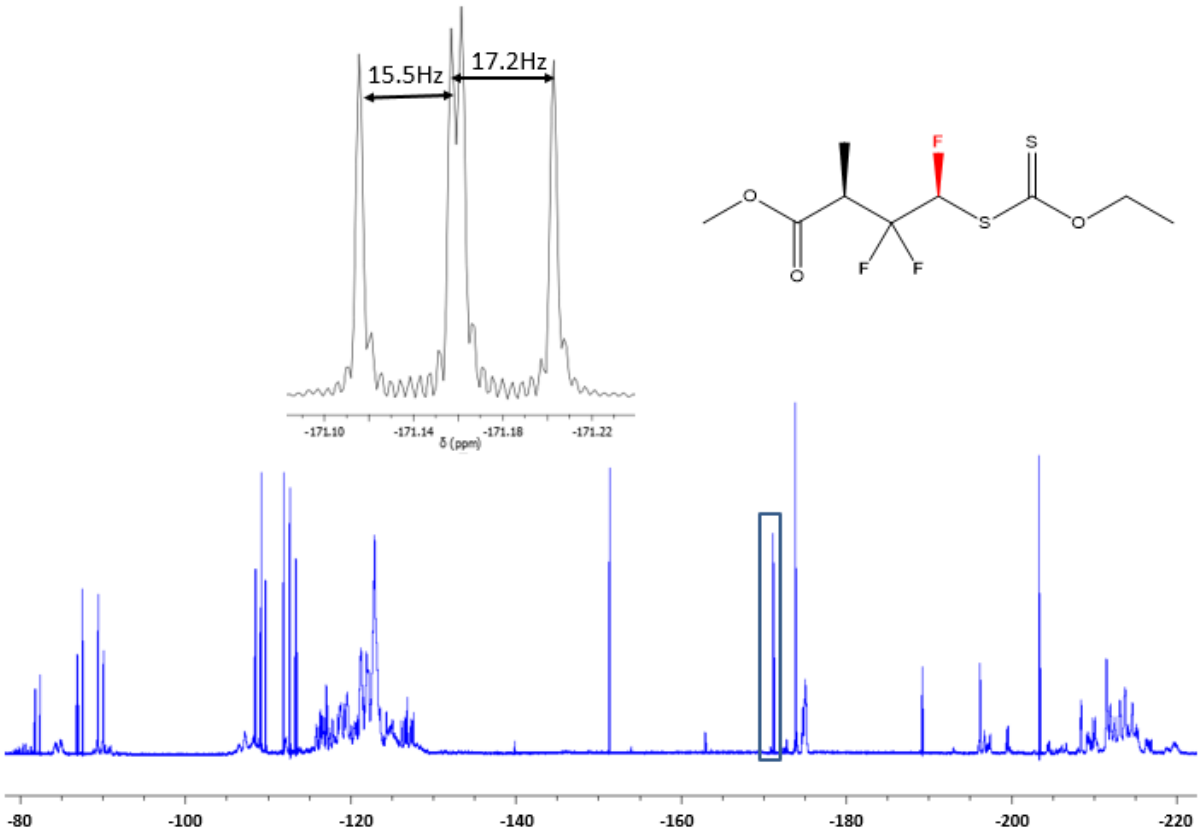

Figure S9. Zoom on $^{19}F\{^{1}H\}$ spectra on the resonance of the CFH from the RS/SR diastereoisomer of the T-adduct (entry 1, Table 1). Only the RS stereoisomer is represented but the splitting pattern is identical for the SR stereoisomer.

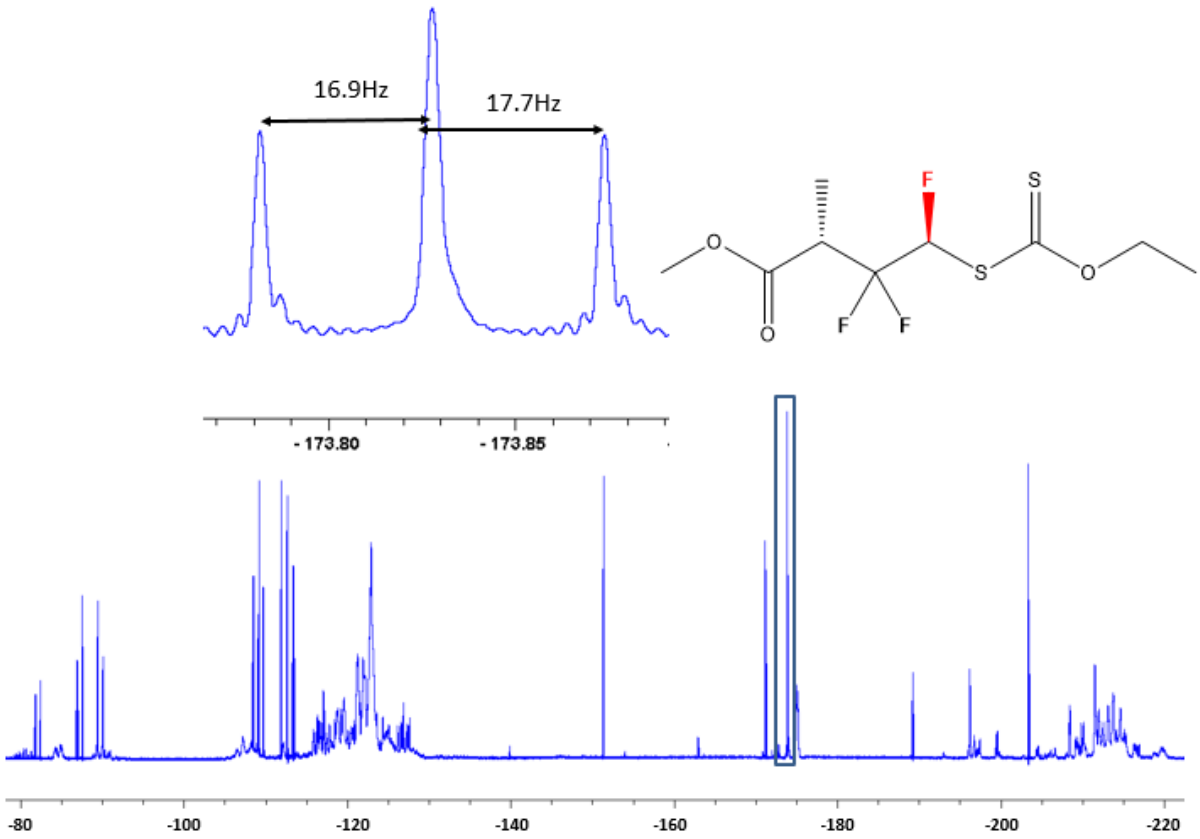

Figure S10. Zoom on $^{19}F\{^{1}H\}$ spectra on the resonance of the CFH from the SS/RR diastereoisomer of the T-adduct (Entry 1, Table 1). Note that the expected doublet of doublet appears as a triplet because of the too small difference of $^{3}J_{F\text{-}F}$ to be seen on the 1D experiment. Only the SS stereoisomer is represented but the splitting pattern is identical for the RR stereoisomer.

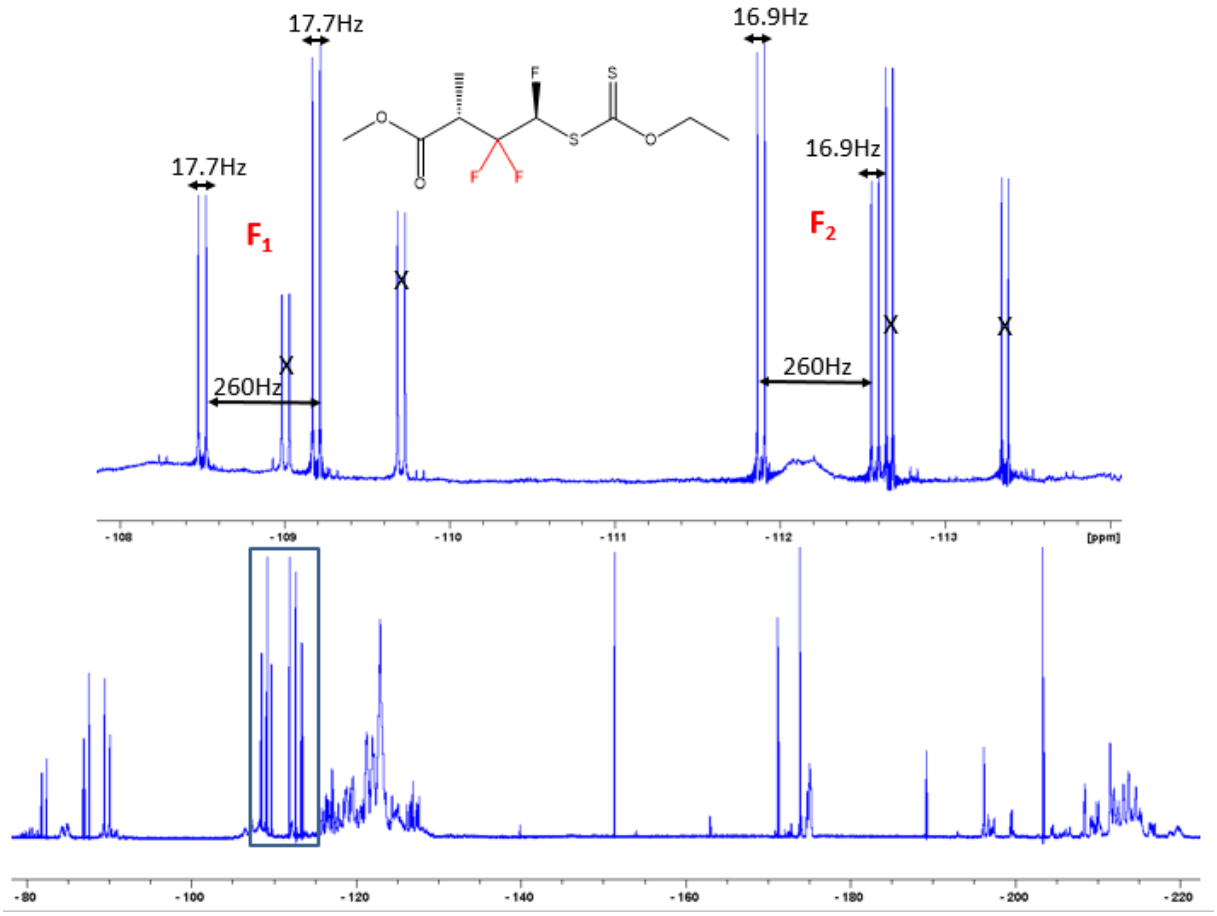

Figure S11. Zoom on $^{19}F\{^{1}H\}$ spectra on the resonance of the CF_2 from the SS/RR diastereoisomer of the T-adduct (Entry 1, Table 1). Only the SS stereoisomer is represented but the splitting pattern is identical for the RR stereoisomer.

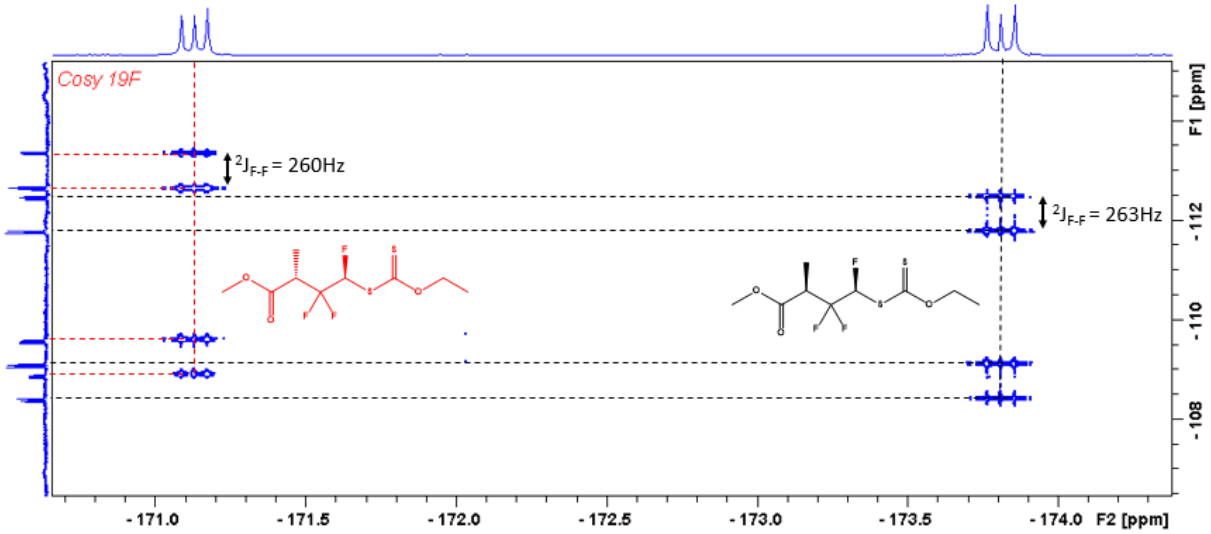

Figure S12. Zoom of the [-106.5 — -115, -179.7 — -174.3] region of the COSY $^{19}F\{^1H\}$ spectrum on the correlations of the T-adducts (Entry 4, Table 1).

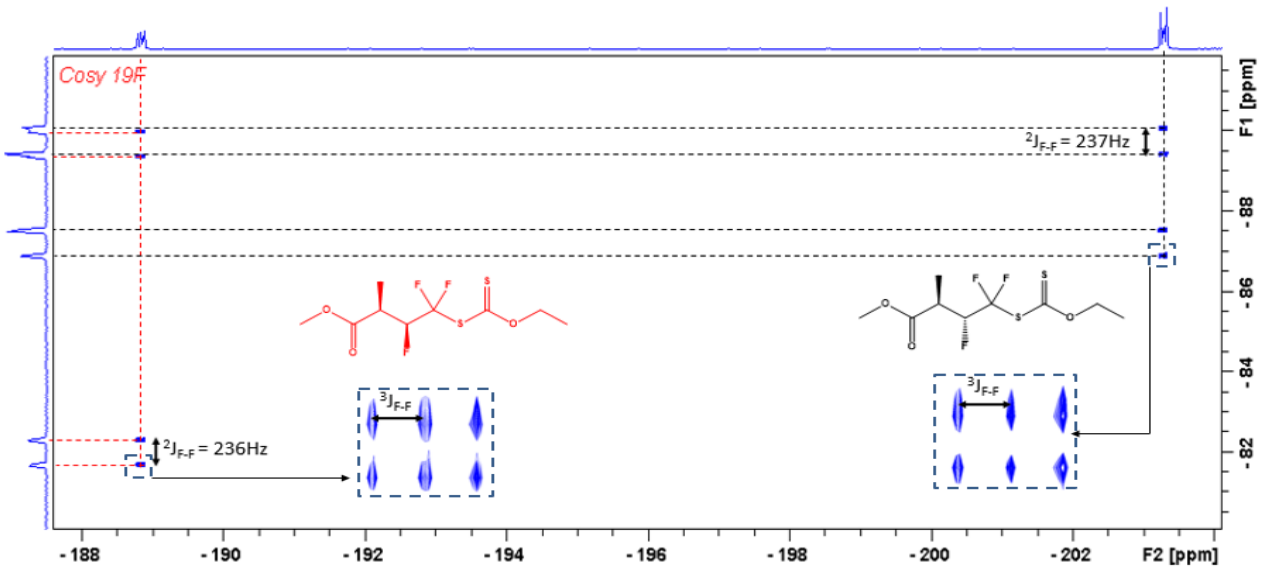

Figure S13. Zoom of the [-80 — -92, -188 — -204] region of the COSY $^{19}F\{^1H\}$ spectrum on the correlations of the H-adducts (Entry 4, Table 1).

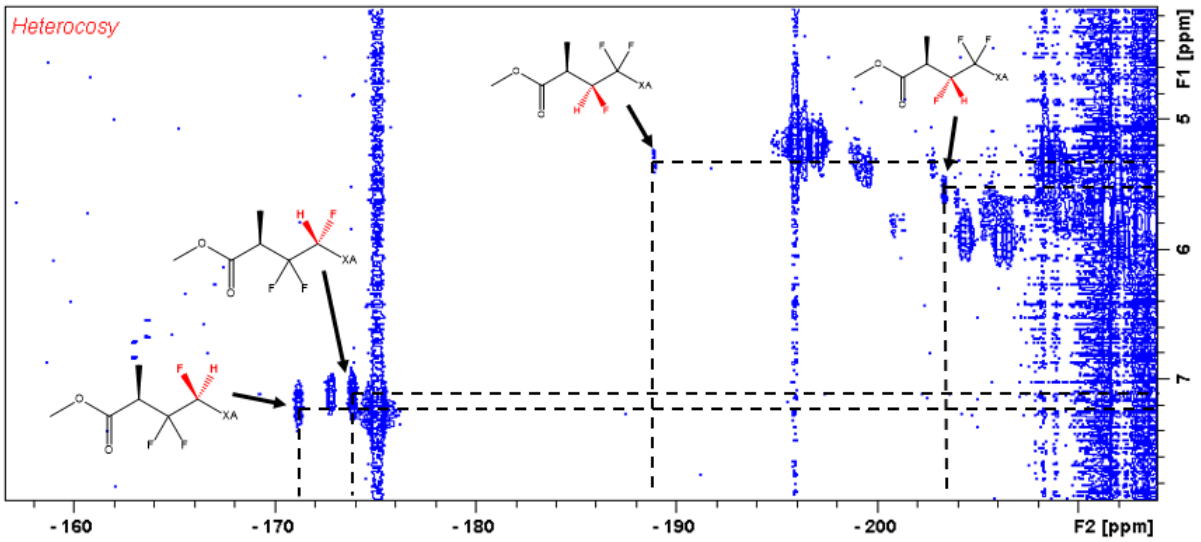

Figure S14. Zoom of the [4.2 — 7.8, -158 — -214] region of the ^{19}F-^{1}H Heterocosy spectrum on the H-F correlations of the CFH groups of T-adduct and H-adducts. (Entry 4, Table 1).

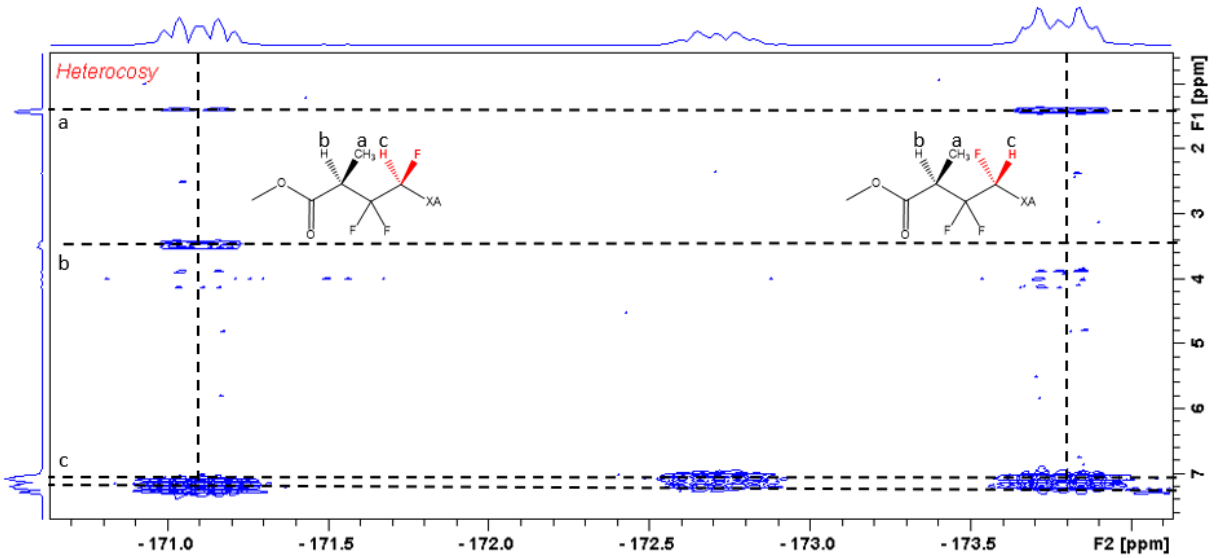

Figure S15. Zoom of the [0.6 — 7.6, -170.7 — -174.2] region of the ^{19}F-^{1}H Heterocosy spectrum on the H-F correlations of the CFH groups of T-adducts. (Entry 4, Table 1).

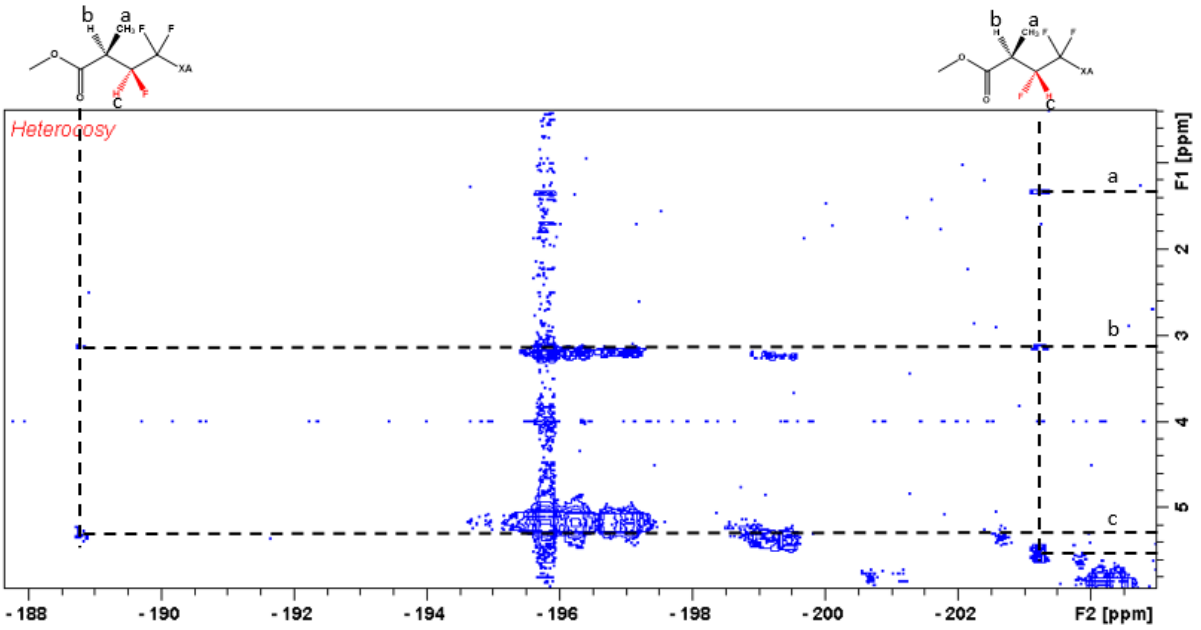

Figure S16. Zoom of the [0.4 — 5.8, -188 — -204.2] region of the ^{19}F-^{1}H Heterocosy spectrum on the H-F correlations of the CFH groups of H-adducts. (Entry 4, Table 1).

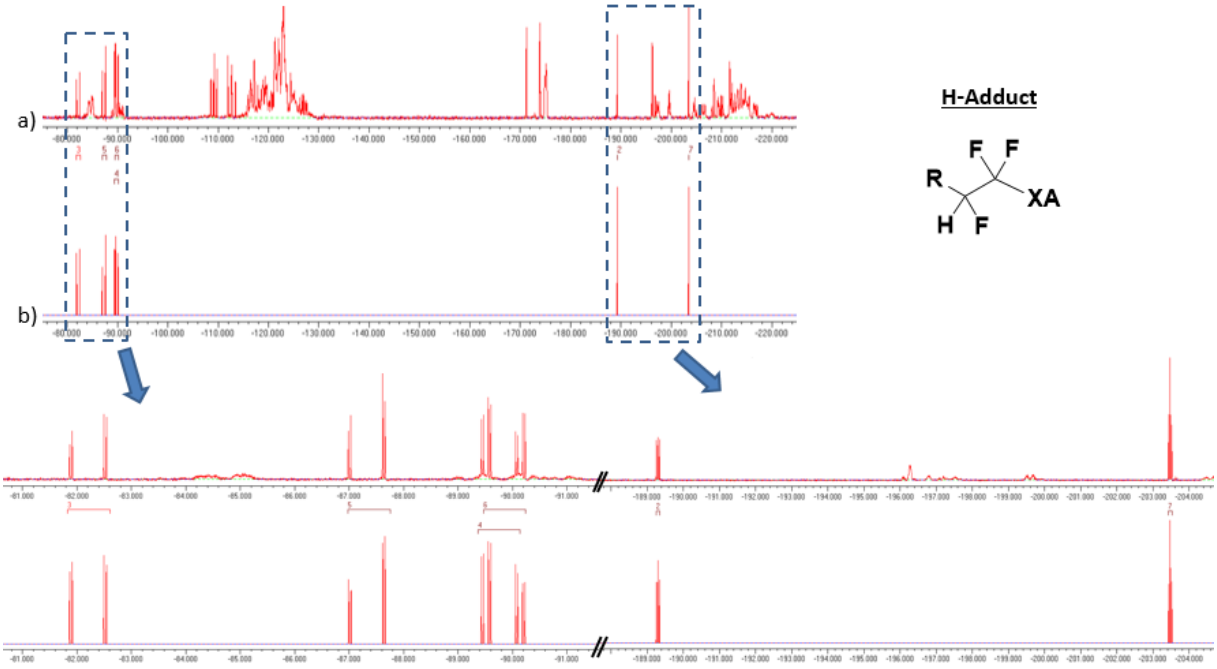

Figure S17. a) experimental $^{19}F\{^{1}H\}$ PTrFE-XA NMR spectrum (Entry 1, Table 1) and b) Simulated $^{19}F\{^{1}H\}$ T-adduct NMR spectrum with gNMR and zoom on the detailed areas of each spectrum.

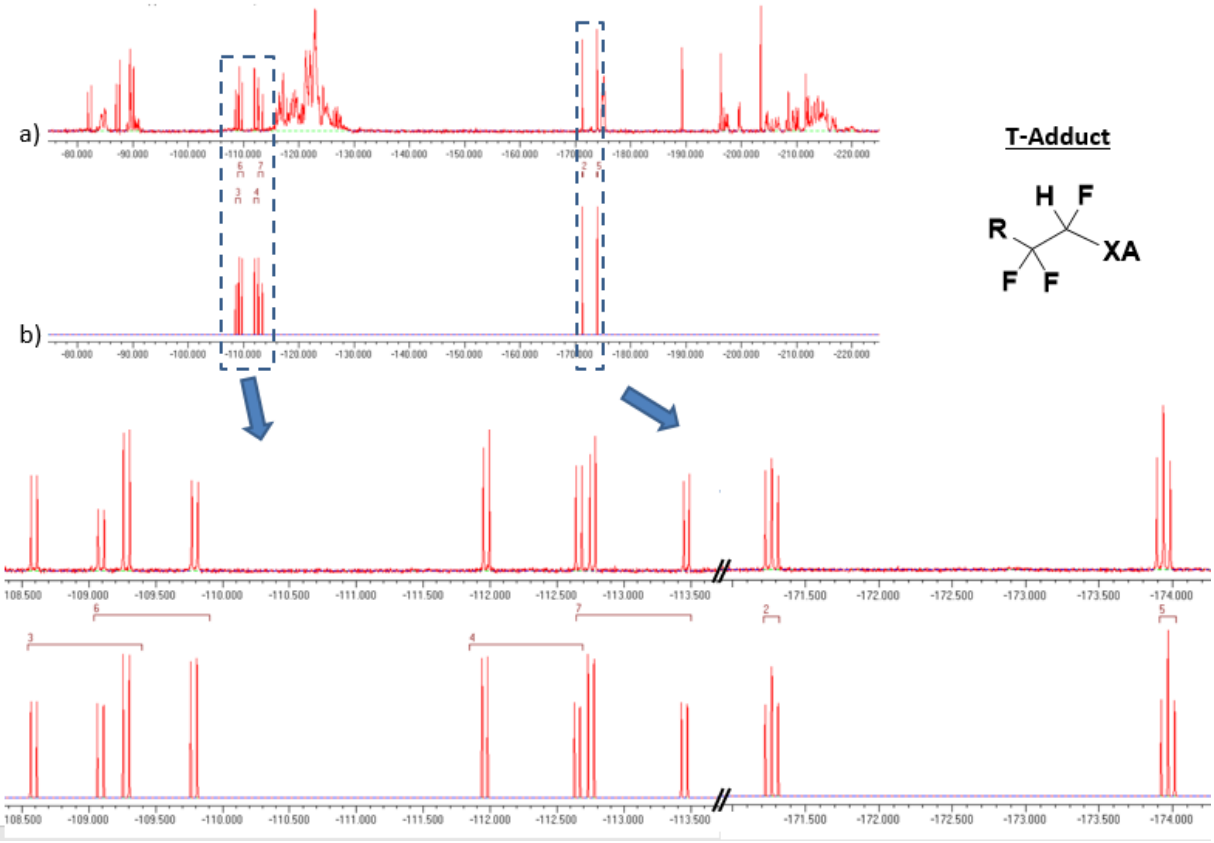

Figure S18. a) experimental $^{19}F\{^{1}H\}$ PTrFE-XA NMR spectrum (Entry 1, Table 1) and b) Simulated $^{19}F\{^{1}H\}$ H-adducts NMR spectrum with gNMR and zoom on the detailed areas of each spectrum.

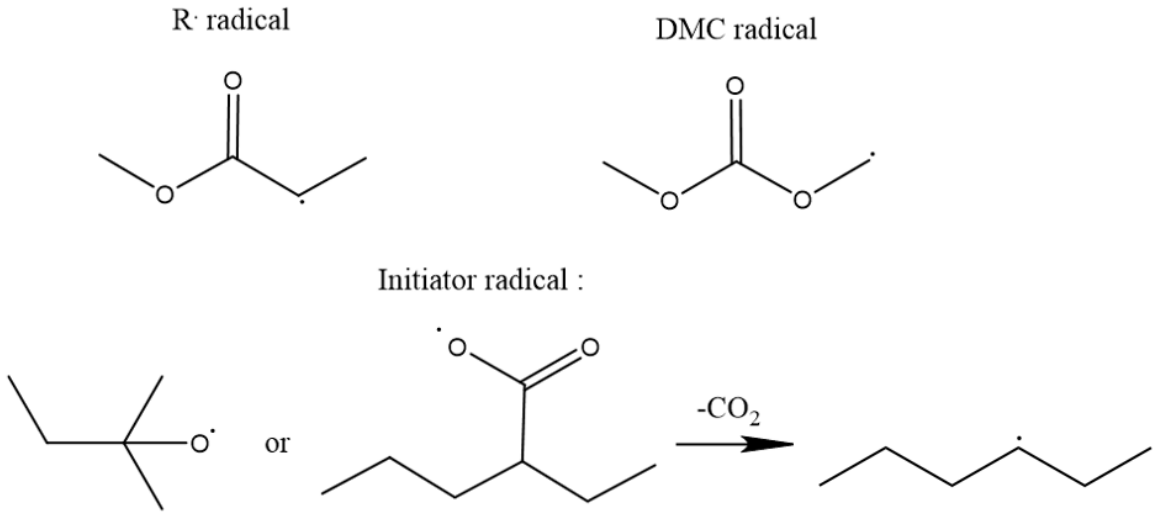

Figure S19. Structure of the different initiating group in the polymerization mixture

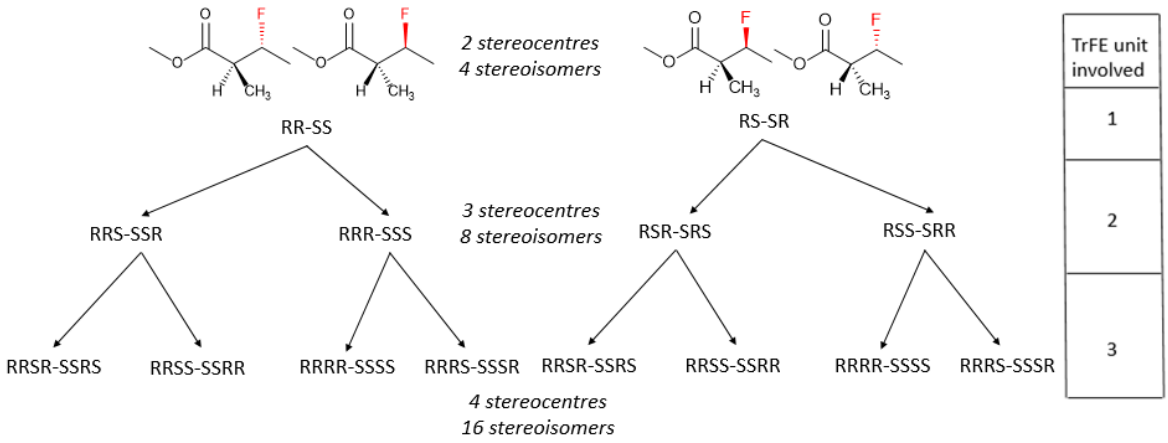

Figure S20. Structures of the regular α-chain-end initiated by the R group of the CTA (R-PTrFE$_T$)

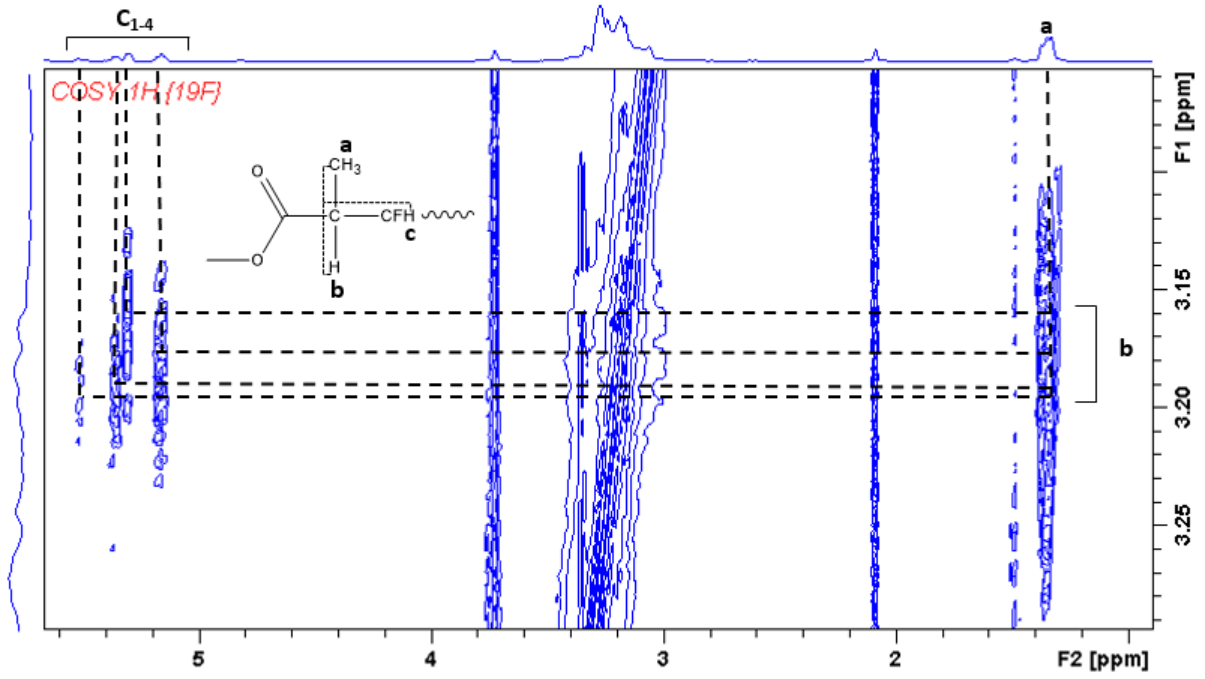

Figure S21. Zoom on the [3.05 - 3.30ppm, 1 - 5.6ppm] region of the COSY $^{1}H\{^{19}F\}$ spectrum of PTrFE made by RAFT recorded in acetone d-6 (Entry 4,Table 1).

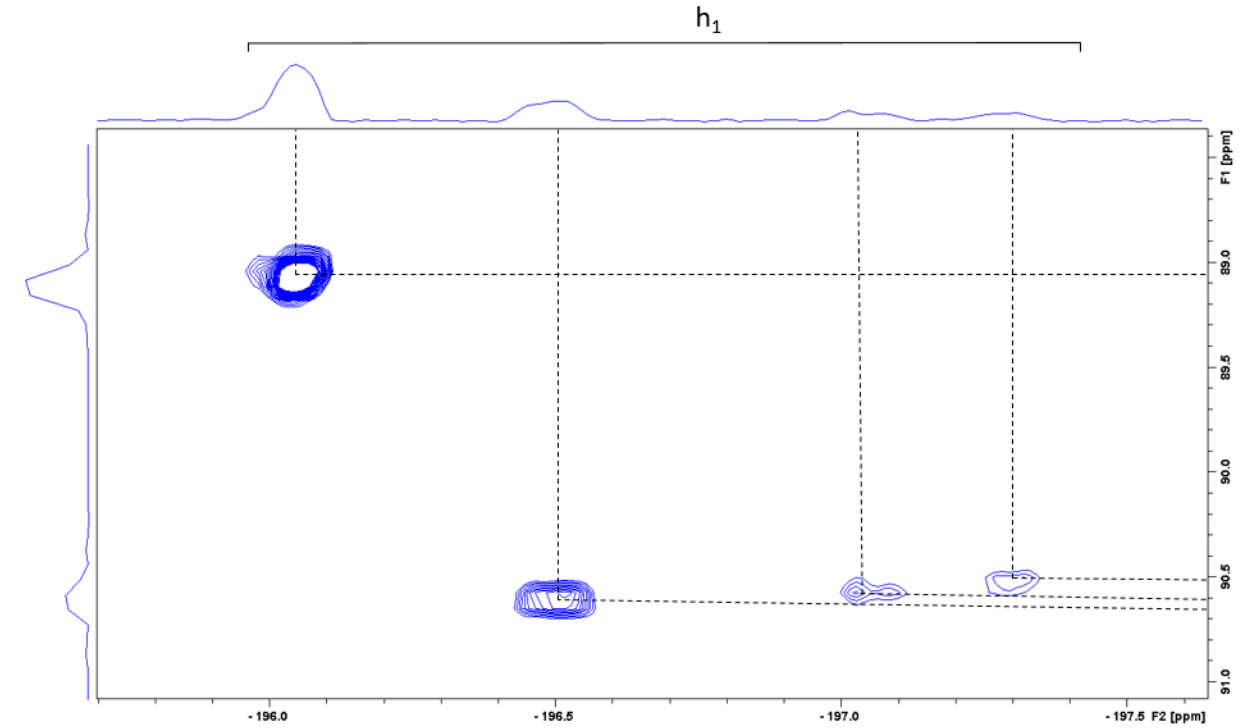

Figure S22. zoom [-195.7 — 197.6ppm; 87.9 — 91ppm] region of the ^{19}F-^{13}C gHSQC spectrum of PTrFE made by RAFT (Entry 4, Table 1) recorded in acetone-d6.

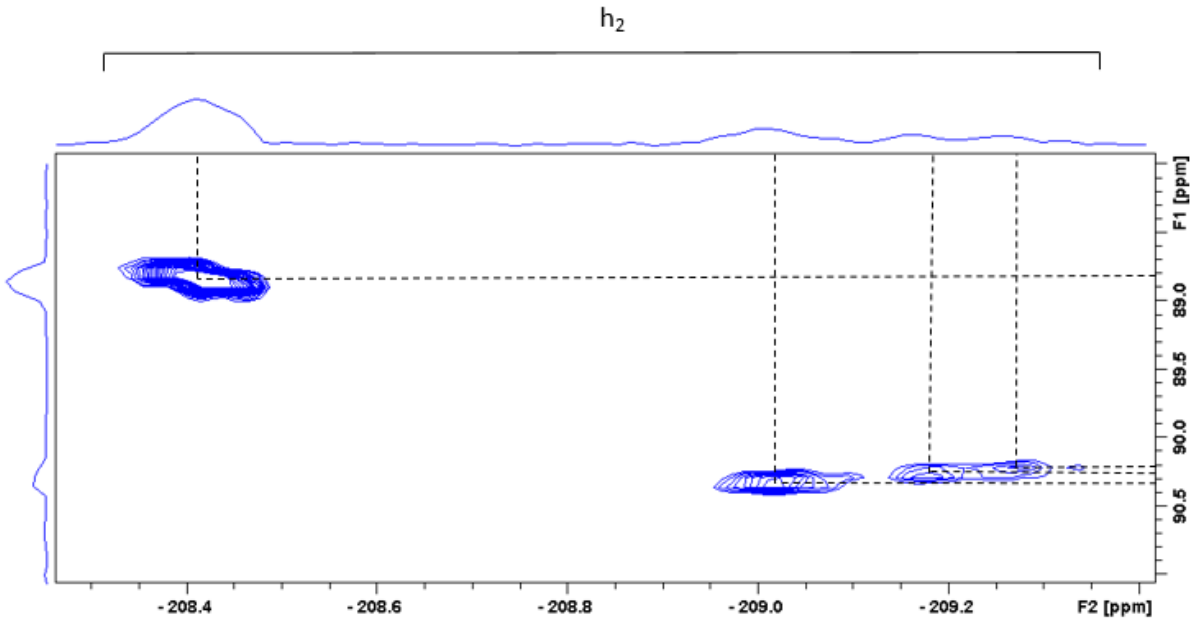

Figure S23. Zoom [-208.3 — -209.4ppm; 88 — 90ppm] region of the ^{19}F-^{13}C gHSQC spectrum of PTrFE made by RAFT (Entry 4, Table 1) recorded in acetone-d6.

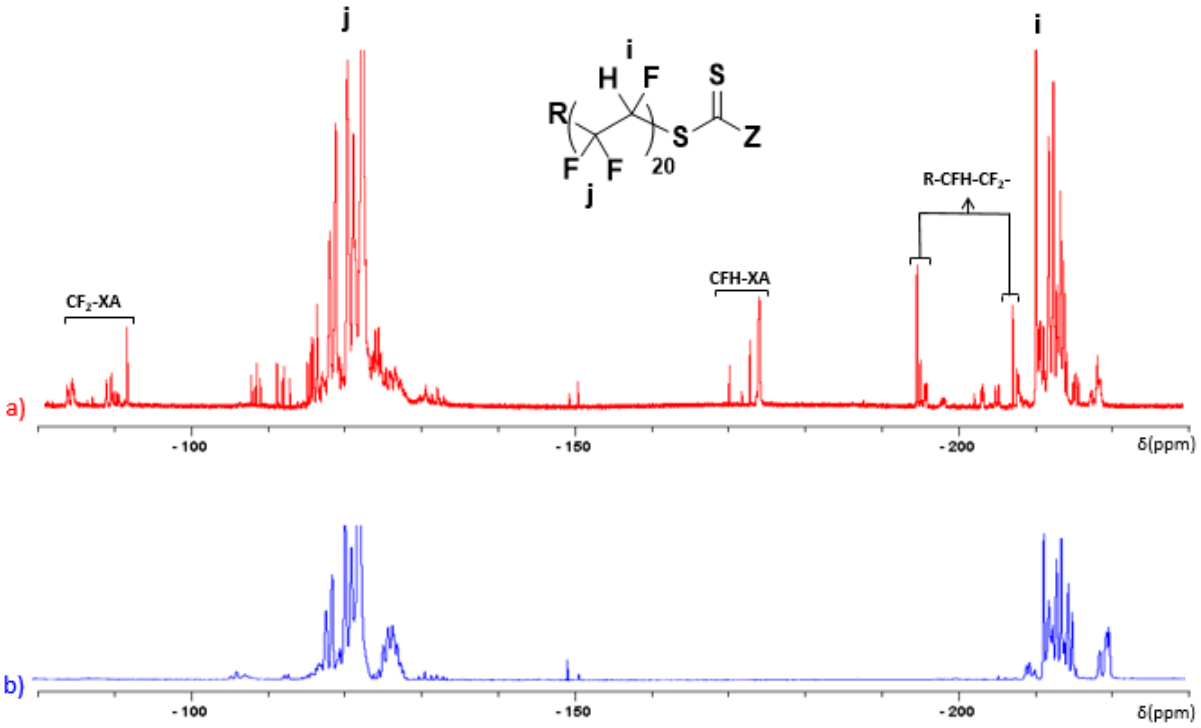

Figure S24. Comparison of the ^{19}F NMR spectra recorded in acetone d-6 of PTrFE prepared by a) RAFT polymerization (Entry 4, Table 1) and b) conventional radical polymerization (Entry 3, Table 1) .

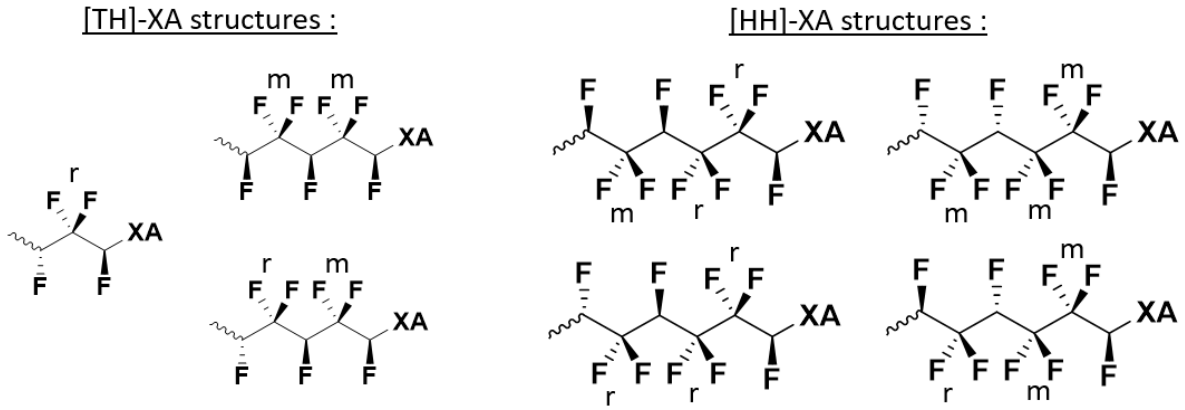

Figure S25. Different possible structures for the -CFH-XA chain end refers to a racemic CF_2 and m refers to a meso CF_2. Note that the respective enantiomers configurations of each chain end is not presented here.

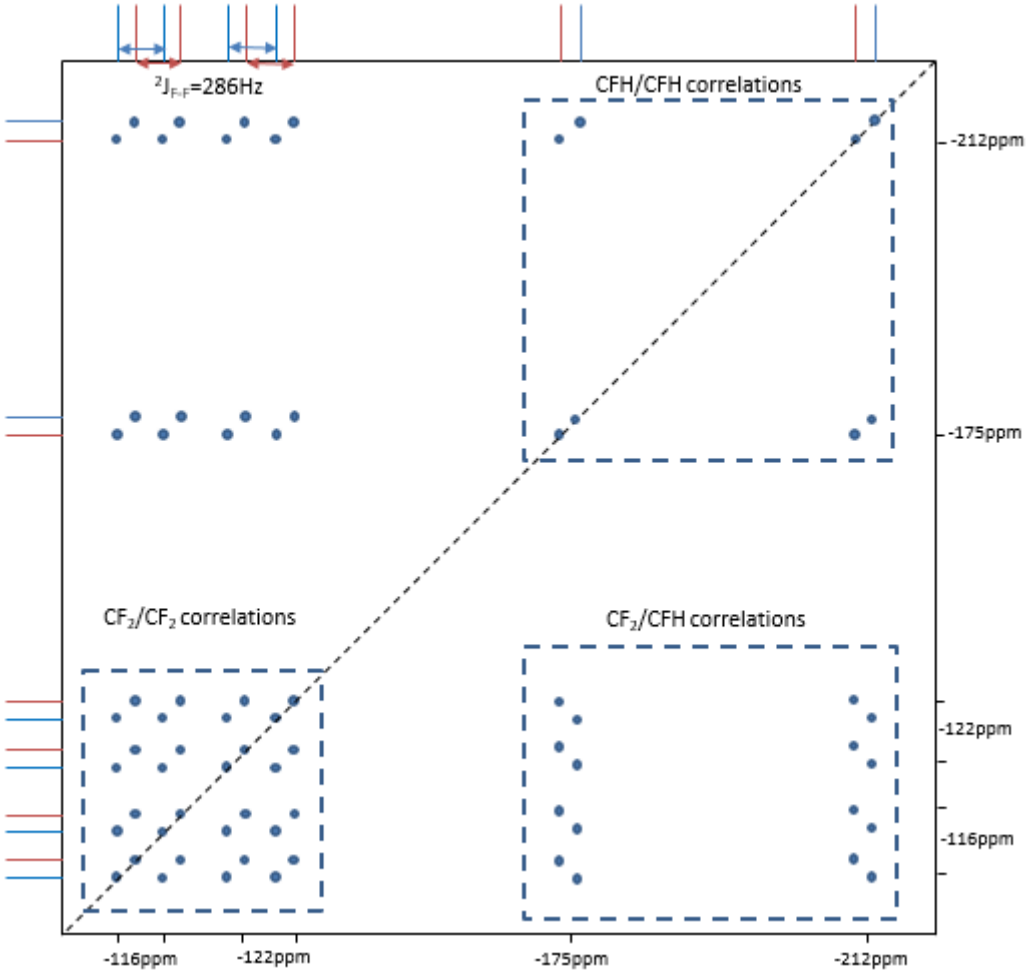

Figure S26. Schematic representation of the correlation system of the two [TH]-XA meso structures.

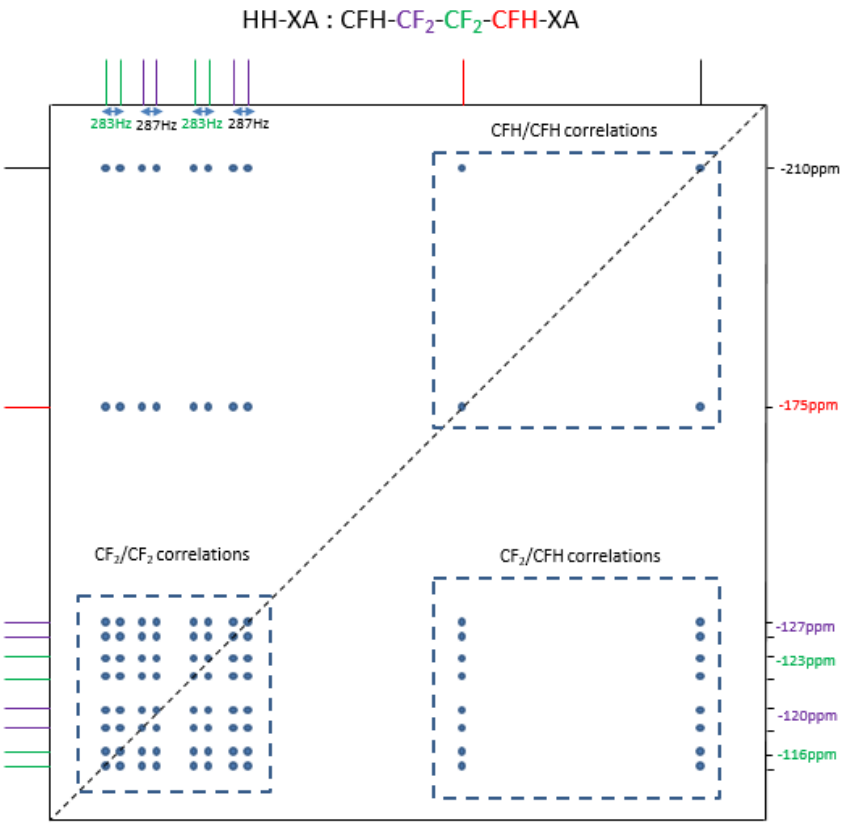

Figure S27. Schematic representation of a typical system of correlation given by [HH]-XA chain end

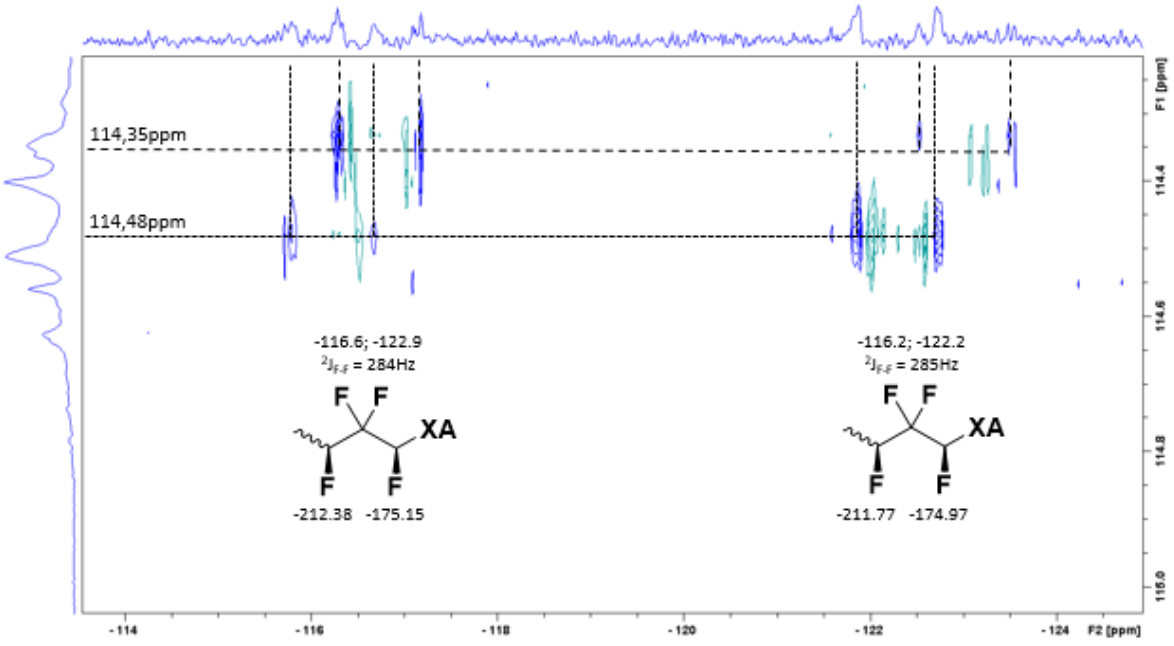

Figure S28. Zoom of the [-113.8 — -124.4ppm; -115.0 — -114.8ppm] region on the gHSQC spectrum of a PTrFE made by RAFT (Entry 4, Table 1) showing the F/C correlations for the CF_2 group of the [TH]-XA chain-end.

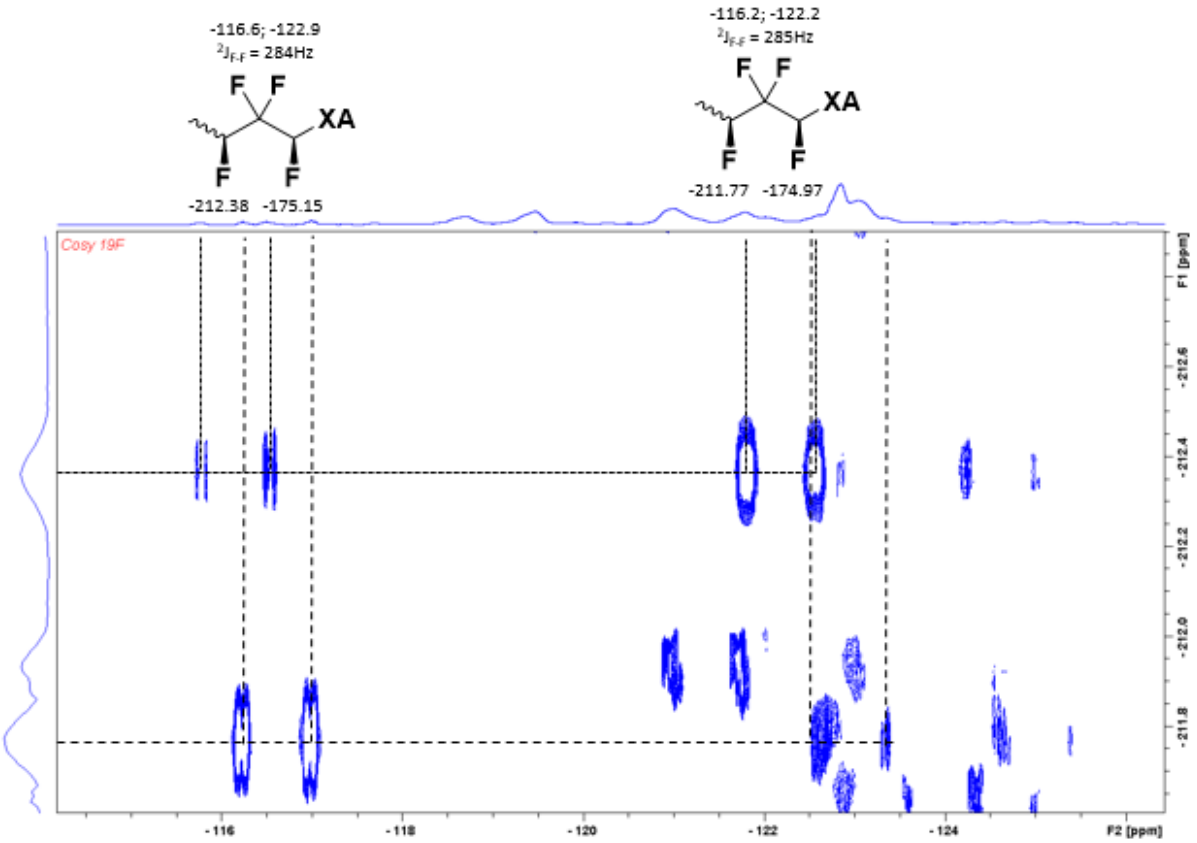

Figure S29. Zoom [-114.2 — 126.5; -211.6 — -212.9] on the ^{19}F COSY spectrum on the CF_2/CFH correlation zone of a PTrFE made by RAFT(Entry 4, Table 1).

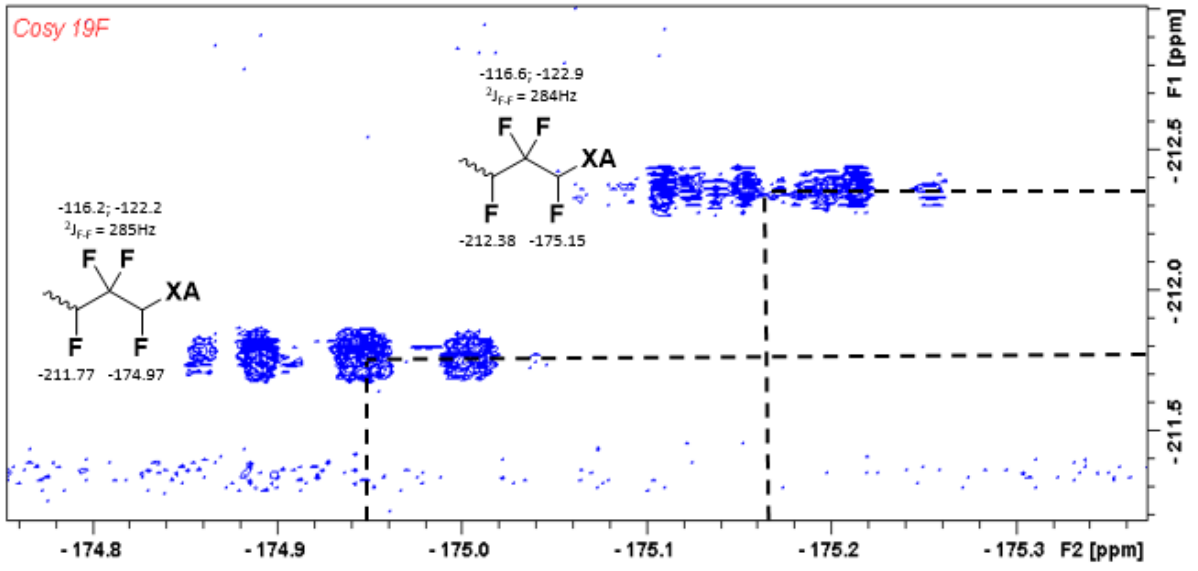

Figure S30. Zoom [-174.8ppm — -175.3 ; -211.2 — -123] on the ^{19}F COSY spectra on the correlation between the ultimate and penultimate CFH group of [HH]-XA chain end of a PTrFE made by RAFT(Entry 4, table 1).

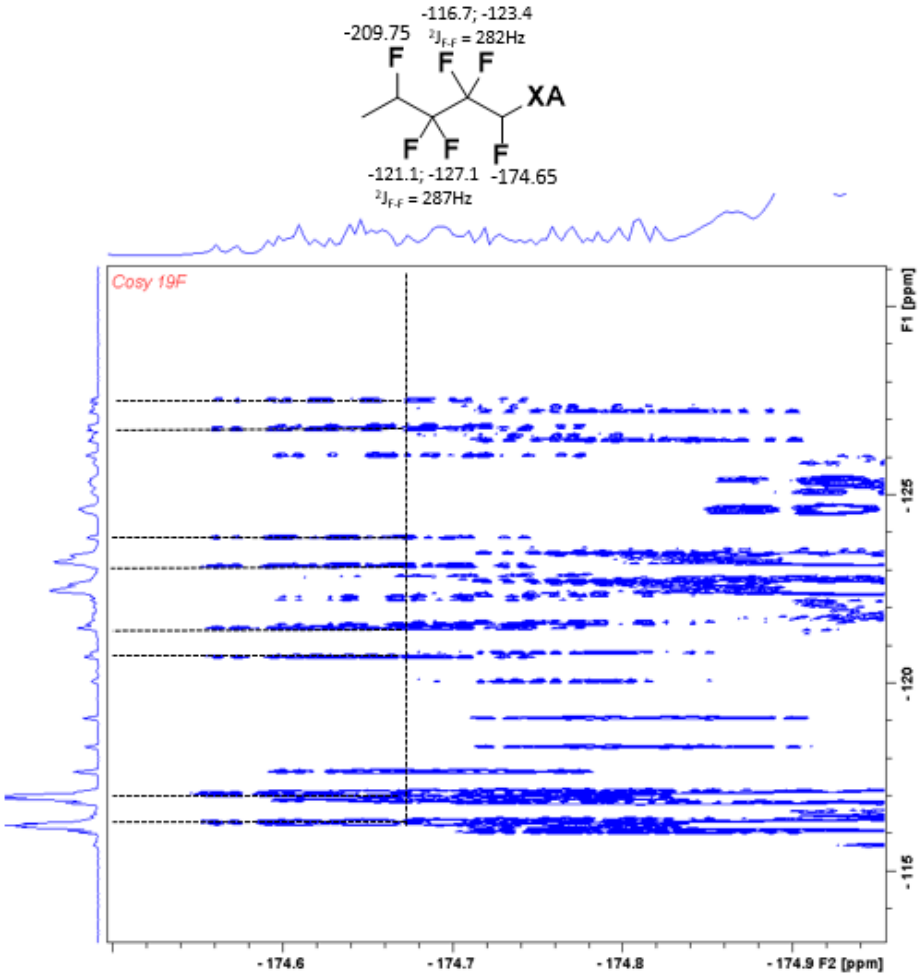

Figure S31. CFH/CF_2 correlation for [HH]-XA chain end of PTrFE made by RAFT

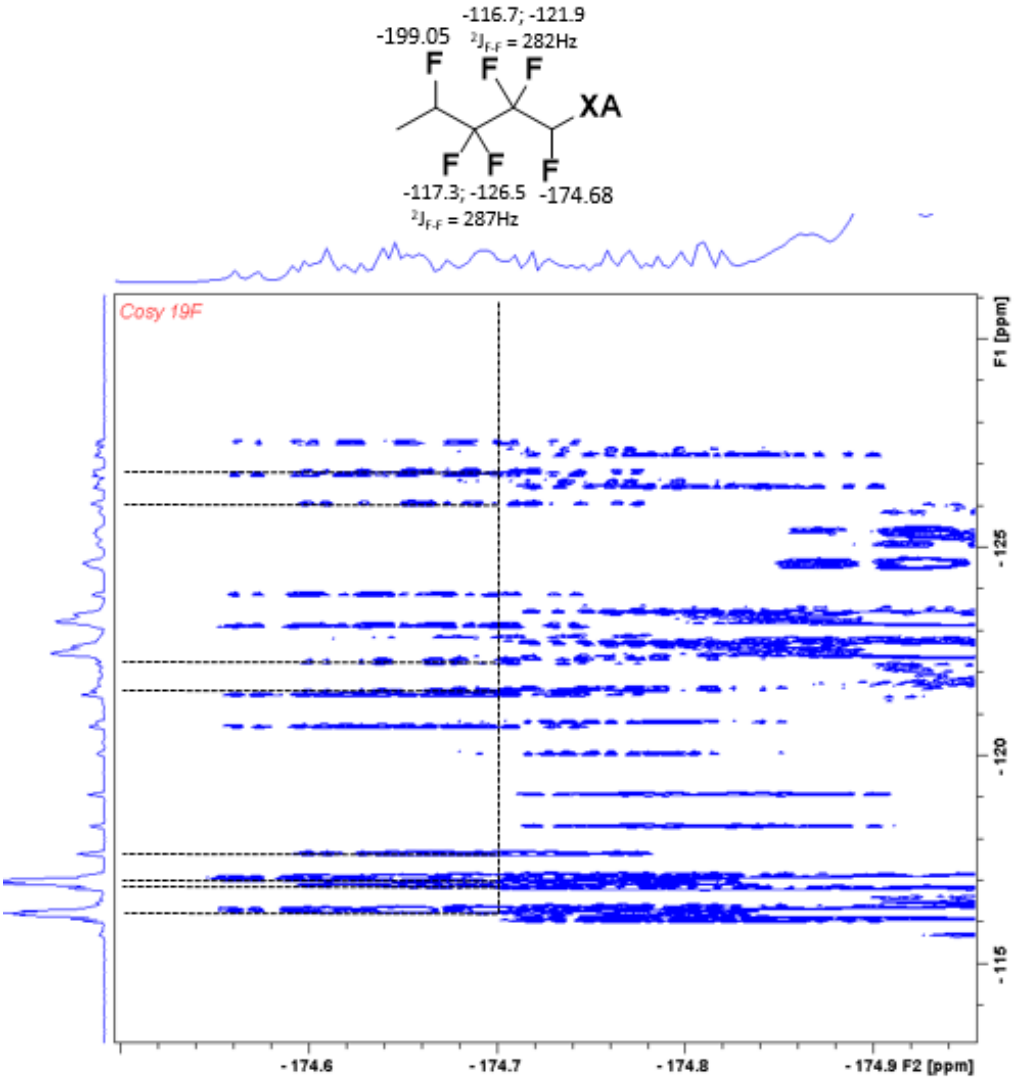

Figure S32. CFH/CF_2 correlation for [HH]-XA chain end of PTrFE made by RAFT.

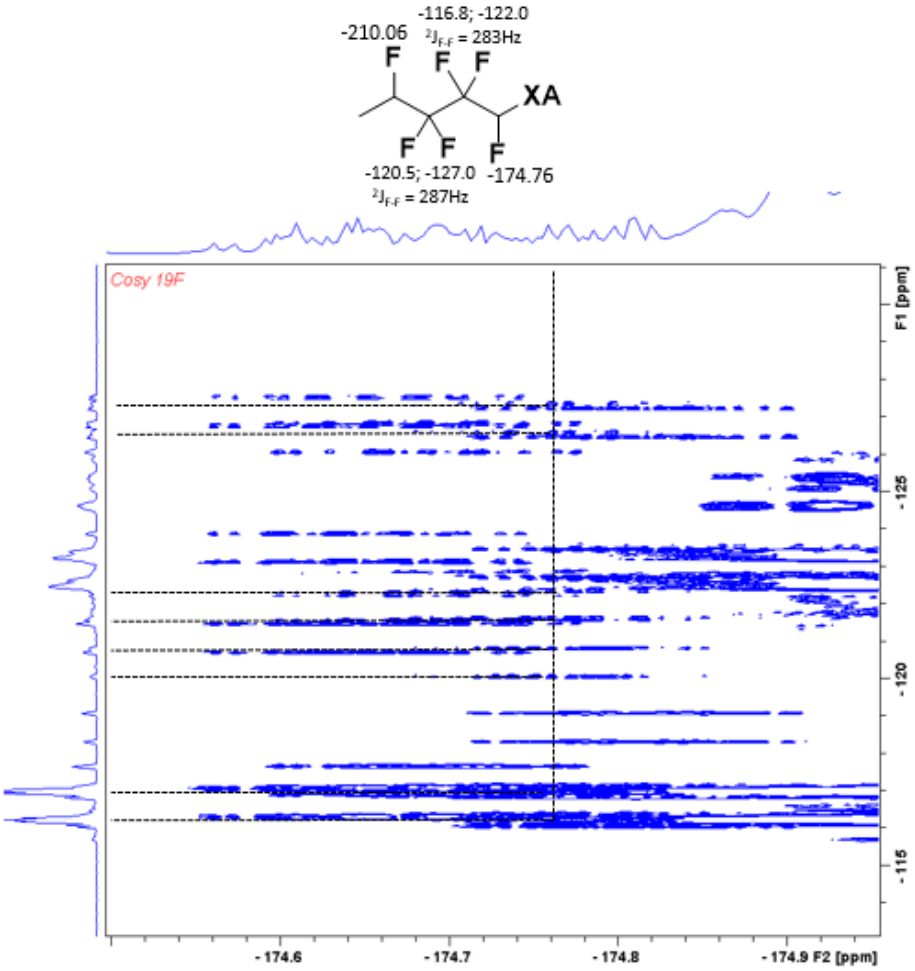

Figure S33. CFH/CF_2 correlation for [HH]-XA chain end of PTrFE made by RAFT.

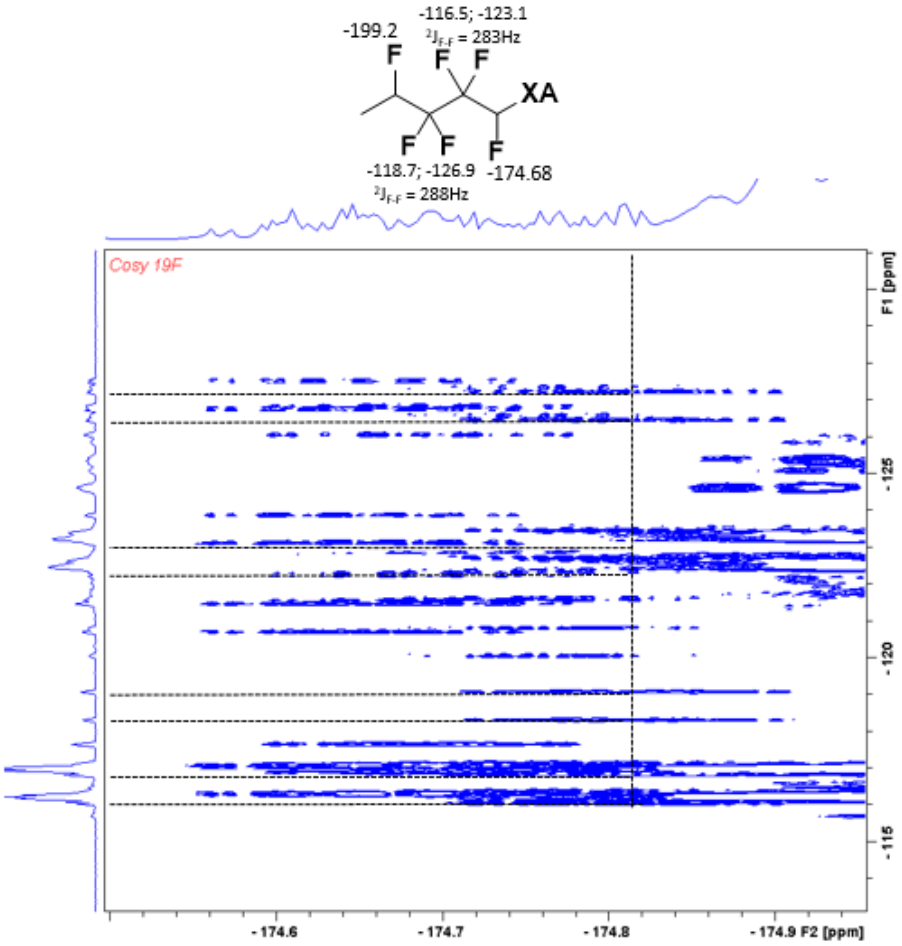

Figure S34. CFH/CF_2 correlation for [HH]-XA chain end of PTrFE made by RAFT.

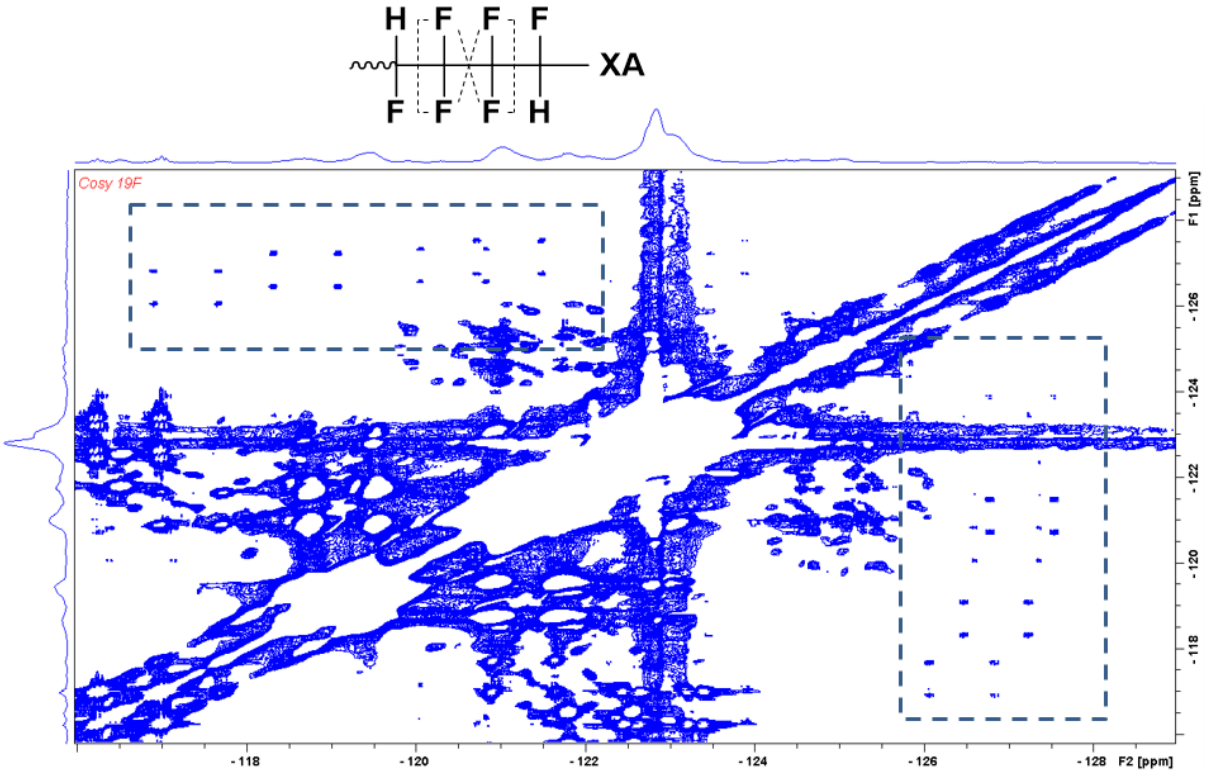

Figure S35. Zoom on the CF_2/CF_2 correlation region of the [HH]-XA chain end of a PTrFE made by RAFT. Boxes show example of a typical CF_2/CF_2 correlation, other correlations are hidden by the strong backbone resonance correlations.

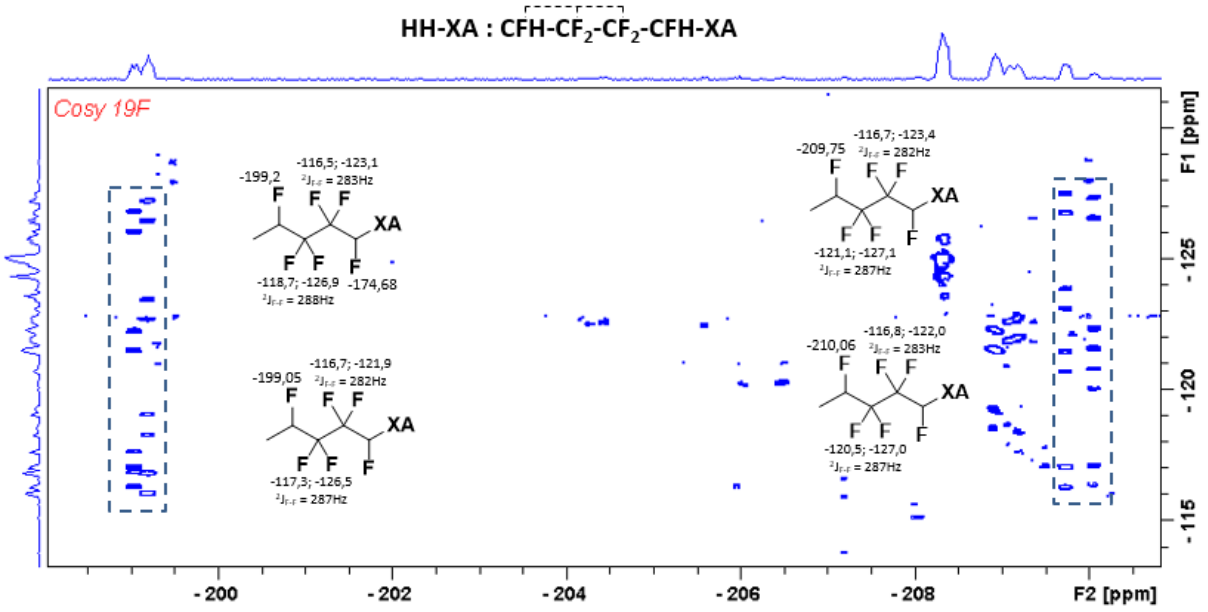

Figure S36. Zoom on the [-198 — -210.2ppm; -114 — -132ppm] region (CF_2/CFH correlations zone) of the ^{19}F COSY spectrum of a PTrFE made by RAFT (Entry 4, Table 1).

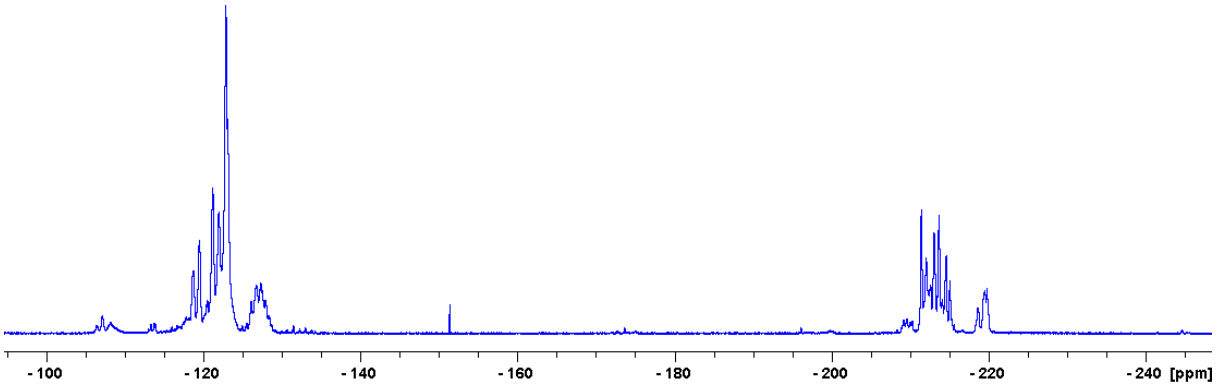

Figure S37 ^{19}F NMR spectra recorded in acetone d-6 of PTrFE prepared by RAFT polymerization (Entry 2, Table 1).

Computational details

The computational work was carried out using the Gaussian09 suite of programs.[1] The geometry optimizations were performed in the gas phase without any symmetry constraint using the B3PW91* functional, which is a reparametrized version of B3PW91 with a reduction of the exact Hartree-Fock exchange from 20% to 15% (c3 parameter reduced from 0.20 to 0.15), similar to what was done for the B3LYP* functional.[2] The 6-31G(d,p) basis functions were used for all atoms. The unrestricted formulation was used for all radicals, yielding negligible spin contamination in all cases. The ZPVE, PV, and TS corrections at 298 K were obtained with Gaussian09 from the solution of the nuclear equation using the standard ideal gas and harmonic approximations at T = 298.15 K, which also verified the nature of all optimized geometries as local minima or first-order saddle points. A correction of 1.95 kcal/mol was applied to all G values to change the standard state from the gas phase (1 atm) to solution (1 M).[3]

Energies (hartrees), views and Cartesian coordinates of all optimized geometries

A. Monomers and radicals

CHF=CF₂ (TrFE)

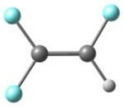

E = -375.95420183
G(298K,1M) = -375.949636

6	0.000000000	0.434876000	0.000000000
6	-0.700700000	-0.694241000	0.000000000
1	-1.783820000	-0.714613000	0.000000000
9	-0.569891000	1.628873000	0.000000000
9	1.317177000	0.508113000	0.000000000
9	-0.081951000	-1.884674000	0.000000000

CH₂=CF₂ (VDF)

E = -276.817941754
G(298K,1M) = -276.804341

6	-1.386768000	0.002088000	0.000517000
6	-0.062812000	0.000473000	-0.000250000
9	0.699065000	1.082140000	0.000097000
9	0.695002000	-1.084340000	-0.000050000
1	-1.924716000	-0.937027000	-0.000253000
1	-1.924408000	0.941462000	-0.001776000

MeCH•(COOMe)

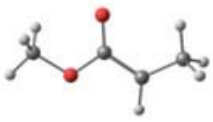

E = -306.752227462
G(298K,1M) = -306.676789

6	2.522248000	0.011936000	0.000019000
6	1.210312000	-0.670792000	-0.000064000
1	2.387007000	1.097354000	0.000137000
1	3.120285000	-0.273745000	-0.878925000
1	3.120264000	-0.273929000	0.878918000
1	1.144850000	-1.756767000	-0.000224000
6	-0.025244000	0.085615000	0.000081000
8	-1.112348000	-0.732262000	-0.000108000
8	-0.107507000	1.307564000	0.000208000
6	-2.365858000	-0.049262000	-0.000105000
1	-3.130488000	-0.829096000	-0.000977000
1	-2.466273000	0.583715000	0.888769000
1	-2.465555000	0.585074000	-0.888080000

CH₃•

E = -39.7940200796
G(298K,1M) = -39.781197

1	1.011496000	-0.390366000	0.000060000
6	0.000051000	-0.000256000	0.000000000
1	-0.844771000	-0.679190000	-0.000160000
1	-0.167031000	1.071094000	0.000100000

B. Acrylate addition to TrFE

B.1 Addition to tail-end

Me(COOMe)CH•---CHFCF₂ (TS)

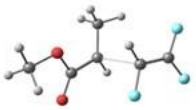

E = -682.695091038
G(298K,1M) = -682.598577

6	-0.104523000	2.120789000	-0.405007000
1	0.960658000	2.377792000	-0.407204000
6	-0.330738000	0.709327000	-0.841822000
6	0.974964000	-0.477956000	0.602582000
6	2.270698000	-0.187762000	0.303620000
9	2.995694000	-0.857482000	-0.568559000
1	0.148713000	0.370539000	-1.758429000
1	0.482813000	0.018923000	1.433021000
9	0.533906000	-1.713637000	0.310795000
9	2.836092000	0.951722000	0.669487000
1	-0.603829000	2.823723000	-1.090262000
1	-0.512379000	2.303201000	0.594503000
6	-1.577861000	0.001654000	-0.569735000
8	-2.037339000	-0.899837000	-1.252151000
8	-2.175159000	0.437039000	0.578068000
6	-3.393188000	-0.236091000	0.900835000
1	-4.137085000	-0.097125000	0.108797000
1	-3.222823000	-1.310559000	1.029769000
1	-3.743421000	0.210701000	1.834128000

Me(COOMe)CH-CHFCF$_2$$^\bullet$ (product)

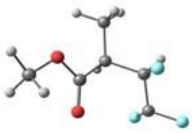

E = -682.74409552
G(298K,1M) = -682.642303

6	0.850318000	2.169720000	0.593659000
1	0.151759000	2.920980000	0.980454000
6	0.218727000	0.780185000	0.659911000
6	-1.053930000	0.717971000	-0.186527000
6	-1.872419000	-0.530575000	0.009533000
9	-2.978274000	-0.569529000	-0.738628000
1	-0.083866000	0.555140000	1.693078000
1	-1.684939000	1.594178000	0.050971000
9	-0.722849000	0.802321000	-1.530651000
9	-2.165664000	-0.780612000	1.291863000
1	1.766950000	2.214450000	1.187514000
1	1.101546000	2.430476000	-0.438852000
6	1.142219000	-0.365685000	0.254021000
8	0.799893000	-1.527967000	0.213293000
8	2.384971000	0.053865000	-0.037841000
6	3.295976000	-0.986018000	-0.419599000
1	3.408419000	-1.714886000	0.389455000
1	2.932122000	-1.504267000	-1.312301000
1	4.244820000	-0.486468000	-0.623164000

B.2 Addition to head-end

Me(COOMe)CH$^\bullet$--- CF$_2$CHF (TS)

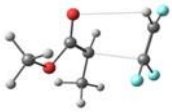

E = -682.69537312
G(298K,1M) = -682.598841

1	-0.658452000	2.586655000	-1.019455000
6	0.305177000	2.092160000	-0.862727000
1	1.003063000	2.485216000	-1.619907000
6	0.178444000	0.611777000	-0.985927000
6	-1.385038000	0.088442000	0.625101000
6	-1.746547000	-1.165421000	0.228395000
9	-2.646378000	-1.284734000	-0.752789000
1	-1.155668000	-2.045366000	0.450337000
9	-0.606703000	0.255635000	1.690431000
9	-2.164757000	1.140571000	0.405425000
1	0.702254000	2.379434000	0.115968000
1	-0.436977000	0.207445000	-1.787106000
6	1.230977000	-0.300344000	-0.544211000
8	1.211653000	-1.514627000	-0.695503000
8	2.236590000	0.343357000	0.102153000
6	3.269683000	-0.509933000	0.596546000
1	2.870843000	-1.219649000	1.329886000
1	3.730961000	-1.077304000	-0.218965000
1	4.002396000	0.150407000	1.065382000

Me(COOMe)CH-CF$_2$CHF$^\bullet$ (product)

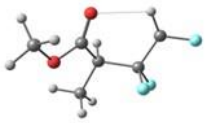

E = -682.747757425
G(298K,1M) = -682.646703

1	1.344335000	2.454393000	-0.889606000
6	0.447014000	2.137436000	-0.351313000
1	0.629552000	2.259696000	0.719705000
6	0.113805000	0.683644000	-0.679480000
6	-1.154138000	0.228752000	0.064536000
6	-1.708116000	-1.072050000	-0.385143000
9	-2.902852000	-1.388893000	0.120456000
1	-1.095795000	-1.895583000	-0.735517000
9	-0.870387000	0.199098000	1.421802000
9	-2.124623000	1.187863000	-0.081622000
1	-0.384641000	2.784984000	-0.640398000
1	-0.106201000	0.581173000	-1.751496000
6	1.239417000	-0.308662000	-0.404441000
8	1.200273000	-1.482756000	-0.716881000
8	2.287005000	0.255819000	0.210667000
6	3.372242000	-0.636958000	0.500755000
1	3.040913000	-1.434397000	1.173153000
1	3.755648000	-1.087297000	-0.420175000
1	4.137382000	-0.023069000	0.978836000

C. Acrylate addition to VDF

C.1 Addition to tail-end

Me(COOMe)CH$^\bullet$---CH$_2$CF$_2$ (TS)

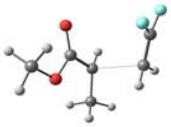

E = -583.559064848
G(298K,1M) = -583.453470

6	-0.489947000	1.302244000	0.525886000
1	0.091263000	1.545905000	1.412742000
6	-2.485283000	-1.600380000	-0.423752000
1	-2.972023000	-1.854393000	0.524247000
1	-3.209687000	-1.622655000	-1.241164000
1	-1.681669000	-2.323244000	-0.602943000
6	1.295282000	0.903298000	-0.768173000
6	1.996358000	-0.171183000	-0.330167000
6	-1.171236000	2.418965000	-0.197966000
1	-0.492099000	3.264742000	-0.361574000
1	-1.567106000	2.090689000	-1.164375000
1	-2.023484000	2.801952000	0.385070000
6	-1.034197000	-0.049004000	0.571591000
8	-0.662224000	-0.923027000	1.341199000
8	-1.972128000	-0.267990000	-0.392724000
9	2.915460000	-0.123754000	0.616518000
9	1.737209000	-1.416092000	-0.681616000
1	0.686937000	0.773598000	-1.656217000
1	1.702781000	1.886522000	-0.562211000

Me(COOMe)CH-CH$_2$CF$_2$$^\bullet$ (product)

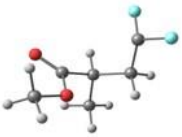

E = -583.599896001
G(298K,1M) = -583.489230

6	-0.147410000	1.150196000	0.143301000
1	0.217363000	1.485202000	1.121021000
6	-2.479066000	-1.657610000	-0.453143000
1	-3.418495000	-1.219599000	-0.100350000
1	-2.618304000	-2.132295000	-1.426370000
1	-2.133823000	-2.388501000	0.285134000
6	1.031506000	0.611550000	-0.676884000
6	1.771777000	-0.480394000	0.023134000
6	-0.830306000	2.324592000	-0.570487000
1	-0.115698000	3.139735000	-0.733568000
1	-1.225483000	2.013456000	-1.544269000
1	-1.659512000	2.715998000	0.028770000
6	-1.172236000	0.069171000	0.451808000
8	-1.682886000	-0.116200000	1.534548000
8	-1.491079000	-0.639670000	-0.653665000
9	2.304189000	-0.141813000	1.207355000
9	2.683708000	-1.116727000	-0.724157000
1	0.677801000	0.217512000	-1.635546000
1	1.731208000	1.437292000	-0.897042000

C.2 Addition to head-end

Me(COOMe)CH•--- CF_2CH_2 (TS)

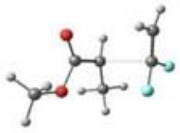

E = -583.553052856
G(298K,1M) = -583.447162

6	-0.129956000	0.666487000	-0.902334000
1	-0.541718000	0.409508000	-1.876062000
6	3.009374000	-0.210095000	0.747866000
1	3.672726000	-0.343420000	-0.113568000
1	3.496203000	0.395246000	1.515483000
1	2.755120000	-1.199025000	1.145056000
6	-1.632795000	-0.467693000	0.291925000
6	-1.619558000	-1.695069000	-0.298895000
6	-0.326924000	2.061499000	-0.406923000
1	-1.352491000	2.401547000	-0.579219000
1	-0.095406000	2.142365000	0.659359000
1	0.345020000	2.754664000	-0.937976000
9	-1.068030000	-0.242754000	1.479601000
9	-2.639181000	0.387516000	0.095134000
1	-2.232760000	-1.861601000	-1.176154000
1	-0.841334000	-2.402656000	-0.044719000
6	1.086991000	-0.090758000	-0.589822000
8	1.398781000	-1.154251000	-1.103327000
8	1.830813000	0.506037000	0.376361000

Me(COOMe)CH-CF_2CH2• (product)

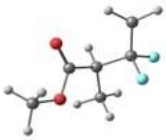

E = -583.598095447
G(298K,1M) = -583.488887

6	-0.325966000	0.441297000	-0.714500000
1	-0.563522000	0.207902000	-1.760972000
6	3.118684000	-0.048666000	0.562258000
1	3.650425000	-0.304444000	-0.359776000
1	3.668796000	0.704769000	1.128736000
1	2.986623000	-0.958090000	1.156954000
6	-1.411250000	-0.253564000	0.131049000
6	-1.636026000	-1.690950000	-0.139577000
6	-0.333862000	1.952485000	-0.493737000
1	-1.305916000	2.364327000	-0.777315000
1	-0.145848000	2.190425000	0.556387000
1	0.440953000	2.433774000	-1.097746000
9	-1.088041000	-0.071919000	1.468351000
9	-2.595921000	0.424006000	-0.052323000
1	-0.850470000	-2.294361000	-0.579212000
1	-2.553202000	-2.139990000	0.228143000
6	1.016739000	-0.229879000	-0.450891000
8	1.309374000	-1.343605000	-0.839528000
8	1.847864000	0.543927000	0.263645000

D. Methyl addition to TrFE

D.1 Addition to tail-end

Me •---$CHFCF_2$ (TS)

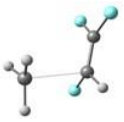

E = -415.741964725
G(298K,1M) = -415.709983

1	1.587362000	2.126268000	0.385735000
6	1.974758000	1.120341000	0.519802000
6	0.407880000	-0.258484000	-0.636776000
6	-0.813451000	-0.008295000	-0.121381000
9	-1.329185000	-0.637926000	0.918015000
1	1.846951000	0.654698000	1.492149000
1	0.727102000	0.215064000	-1.557685000
9	1.028522000	-1.406371000	-0.308376000
9	-1.524136000	1.049981000	-0.479627000
1	2.846655000	0.831445000	-0.060172000

Me-$CHFCF_2$• (product)

E = -415.814267788
G(298K,1M) = -415.774433

6	-0.658724000	-0.132452000	0.322260000
6	0.721545000	0.049162000	-0.252555000
9	1.588031000	-0.917293000	0.051907000
1	-0.574918000	-0.224050000	1.420633000
9	-1.145763000	-1.340998000	-0.154489000
9	1.258432000	1.253981000	-0.018450000
6	-1.599599000	0.992046000	-0.052464000
1	-1.236977000	1.945422000	0.344269000
1	-1.681559000	1.072055000	-1.141305000
1	-2.592188000	0.792824000	0.362243000

D.2 Addition to head-end

Me•---CF_2CHF (TS)

E = -415.740974472
G(298K,1M) = -415.708694

1	2.182819000	1.229612000	0.401875000
6	1.317950000	1.611703000	-0.132360000
6	0.150263000	-0.449063000	-0.009045000
6	-1.022114000	-0.171853000	-0.622098000
9	-2.003266000	0.430511000	0.063990000
1	-1.154651000	-0.235984000	-1.695454000
9	1.090588000	-1.149550000	-0.634343000
9	0.274119000	-0.498773000	1.310172000
1	0.620470000	2.237895000	0.415742000
1	1.421797000	1.784060000	-1.199521000

Me-CF_2CHF• (product)

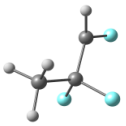

E = -415.816098186
G(298K,1M) = -415.777718

6	-1.613888000	0.818085000	-0.185336000
6	-0.367361000	-0.013806000	-0.001515000
6	0.888783000	0.779920000	-0.038526000
9	2.028413000	0.086562000	-0.045119000
1	0.964185000	1.786968000	0.365160000
9	-0.458548000	-0.695754000	1.201202000
9	-0.306762000	-0.983852000	-0.970180000
1	-1.599750000	1.317465000	-1.158517000
1	-1.694017000	1.570610000	0.605326000
1	-2.483544000	0.157154000	-0.132828000

[1] M. J. Frisch, G. W. Trucks, H. B. Schlegel, G. E. Scuseria, M. A. Robb, J. R. Cheeseman, G. Scalmani, V. Barone, B. Mennucci, G. A. Petersson, H. Nakatsuji, M. Caricato, X. Li, H. P. Hratchian, A. F. Izmaylov, J. Bloino, G. Zheng, J. L. Sonnenberg, M. Hada, M. Ehara, K. Toyota, R. Fukuda, J. Hasegawa, M. Ishida, T. Nakajima, Y. Honda, O. Kitao, H. Nakai, T. Vreven, J. A. Montgomery Jr., J. E. Peralta, F. Ogliaro, M. Bearpark, J. J. Heyd, E. Brothers, K. N. Kudin, V. N. Staroverov, R. Kobayashi, J. Normand, K. Raghavachari, A. Rendell, J. C. Burant, S. S. Iyengar, J. Tomasi, M. Cossi, N. Rega, N. J. Millam, M. Klene, J. E. Knox, J. B. Cross, V. Bakken, C. Adamo, J. Jaramillo, R. Gomperts, R. E. Stratmann, O. Yazyev, A. J. Austin, R. Cammi, C. Pomelli, J. W. Ochterski, R. L. Martin, K. Morokuma, V. G. Zakrzewski, G. A. Voth, P. Salvador, J. J. Dannenberg, S. Dapprich, A. D. Daniels, Ö. Farkas, J. B. Foresman, J. V. Ortiz, J. Cioslowski, D. J. Fox, *Gaussian 09, Revision D.01*, Gaussian, Inc., Wallingford CT, **2009**.

[2] (a) M. Reiher, *Inorg. Chem.* **2002**, *41*, 6928-6935. (b) O. Salomon, M. Reiher, B. A. Hess, *J. Chem. Phys.* **2002**, *117*, 4729-4737.

[3] V. S. Bryantsev, M. S. Diallo, W. A. Goddard, III, *J. Phys. Chem. B* **2008**, *112*, 9709-9719.